Preferred citation: R. Farnood. Review: Optical properties of paper: theory and practice. In **Advances in Pulp and Paper Research, Oxford 2009**, *Trans. of the XIVth Fund. Res. Symp. Oxford, 2009*, (S.J. I'Anson, ed.), pp 273–352, FRC, Manchester, 2018. DOI: 10.15376/frc.2009.1.273.

OPTICAL PROPERTIES OF PAPER: THEORY AND PRACTICE

Ramin Farnood

Department of Chemical Engineering and Applied Chemistry
University of Toronto, February 25, 2009, Revised: May 22, 2009

ABSTRACT

The perceived value of paper products depends not only upon their performance but also upon their visual appeal. The optical properties of paper, including whiteness, brightness, opacity, and gloss, affect its visual perception and appeal. From a practical point of view, it is important to quantify these optical properties by means of reliable and repeatable measurement methods, and furthermore, to relate these measured values to the structure of paper and characteristics of its constituents. This would allow papermakers to design new products with improved quality and reduced cost. In recent years, significant progress has been made in terms of the fundamental understanding of light-paper interaction and its effect on paper's appearance. The introduction of digital imaging technology has led to the emergence of a new category of optical testing methods and has provided fresh insights into the relationship between paper's structure and its optical properties. These developments were complemented by advances in the theoretical treatment of light propagation in paper. In particular, wave scattering theories in random media are finding increasing applicability in gaining a better understanding of the optical properties of paper. In this document, a review of these advancements is presented.

INTRODUCTION

The perceived value of paper products depends on both their performance and their appearance. The appearance of paper, like that of any other material, is dependent on its interaction with visible light, and therefore is not only a function of paper characteristics, but is also influenced by the illumination conditions and observer's response. The growing demand for a higher quality paper together with reduced fibre supply and market pressures have led to significant changes in papermaking practices. To address these challenges, it is even more important to develop a fundamental understanding of factors that influence the optical properties and appearance of paper. In this document, a review of recent advances in characterization and theoretical analysis of paper optical properties is presented with a focus on whiteness, brightness, opacity and gloss.

Commission Internationale de l'Éclairage (CIE) defines brightness as "the reflectance of blue light with a specified spectral distribution peaking at 457 nm compared to that of a perfectly reflecting, perfectly diffusing surface" [1]. This is a useful and sensitive measure of the progression of the bleaching process [2]. Historically, brightness has been used as a measure of "whiteness" of paper. However, the illuminant prescribed for brightness measurement differs significantly from typical illumination conditions that form the basis for common perceptions of paper quality. In recent years, the introduction of new paper products containing optical brightening agents (OBA) has created further ambiguity in evaluating brightness and whiteness [2]. Therefore, a great deal of effort has been dedicated to a better quantification of the whiteness of paper through the use of suitable illuminants that mimic indoor lighting conditions, and to provide papermakers with improved testing methods to assess the whiteness of paper [3–5]. Whiteness measured in this way differs fundamentally from paper brightness in that whiteness includes the entire visible spectrum in its assessment; therefore, it is a better predictor of the subjective ranking of paper than brightness [3].

Opacity is the attribute of paper that makes it impermeable to rays of light. This property can be quantified as the ratio of the reflectance of a single sheet of paper with a black backing to that of a pad of the same sample [6]. Although opacity is determined through reflectance tests, it is related to the ability of paper to hide what is printed behind it. Over the past decade, with the escalating cost and reduced availability of fibre resources, there is an increasing desire to lower paper grammage while maintaining adequate paper opacity.

Gloss refers to the degree of paper's "shininess" and is related to the ability of paper to reflect light in the specular direction. Gloss is a psychophysical

property that significantly influences the visual perception of the observer. With the rapid penetration of information technology and electronic media into the market, there has been a pressing demand to develop high quality products with improved paper and print gloss. This has been achieved largely through the implementation of modern coating and finishing technologies. Therefore, fundamental understanding of gloss and factors that contribute to it have attracted increasing attention in recent years.

In the sections that follow, an overview of optical testing of paper will be presented and theoretical background for light reflection and scattering from surfaces will be discussed. Following these sections, a detailed account of recent advances in our understanding of the optical properties of paper including whiteness, brightness, opacity and gloss will be provided. Finally, effects of papermaking furnish – particularly pigments and fillers – on paper's optical properties will be reviewed.

OPTICAL TESTING OF PAPER

Quantitative characterization of the interaction of light with paper is important not only for papermaking practitioners, but also for researchers who study the optical properties of pulp, paper and print. Instruments used for the measurement of optical properties of paper can be classified as spectrophotometers, goniophotometers, microdensitometers, glossmeters, colorimeters, and image analysis systems. Great care has been taken in the design and construction of these pieces of equipment in terms of optical geometry and spectral characteristics to ensure relevant and stable quantification of optical properties. An overview of conventional measurement devices for the optical properties of paper can be found elsewhere [7–9]. In the following sections, the role of the illuminant in the perceived paper appearance is discussed. In addition, brief overviews of standard methods, as well as new laboratory techniques for the optical testing of paper, are presented.

Luminosity function and illuminant

The standard measurement techniques discussed earlier were developed to "quantify" the response of a human observer in terms of paper appearance. This response depends on the sensitivity of human eye to light as characterized by the luminosity function. The luminosity function represents the average sensitivity of human eye to various wavelengths of light. In principle, a standard luminosity function should be applicable over a wide range in terms of luminance and chromaticity. However, in practice, the luminosity function

is only accurate for the test condition under which it is determined [10]. The most commonly used luminosity function was originally recommended by the CIE in 1924 and was later modified by D.B. Judd in 1951 and J.J. Vos in 1978 [11]. Most recently, Sharpe *et al.* revisited this topic and obtained an improved relationship for standard daylight conditions [10]. The modified CIE luminosity function and Sharpe's improved function are given in Figure 1. It is particularly important to notice the difference between the functions in the blue region that, as discussed later in this article, can have a significant impact on the perceived whiteness of paper.

Since the sensitivity of human eye is wavelength dependent, illumination conditions – and in particular the spectral output of the light source – are important factors in defining the appearance of paper. Figure 2 underscores

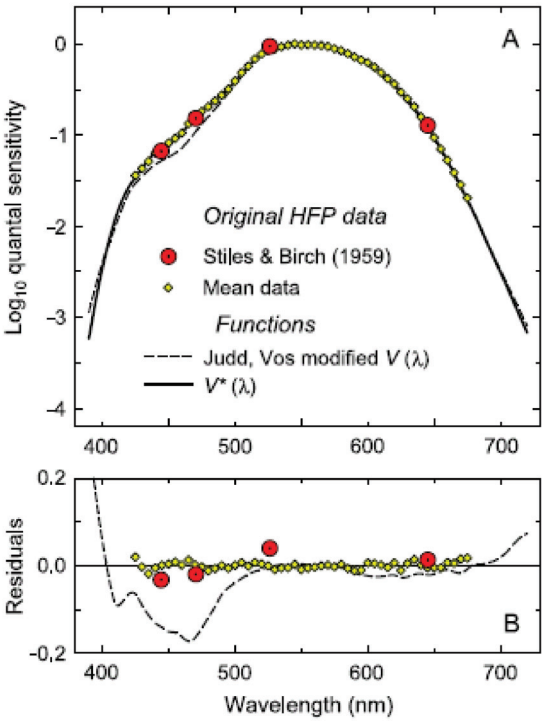

Figure 1. A) Sharpe's luminosity function (solid line) and Judd-Vos modified CIE luminosity function (dashed curve). Diamonds represent the experimental data. (B) Differences between Sharpe's function and Judd-Vos' function [10].

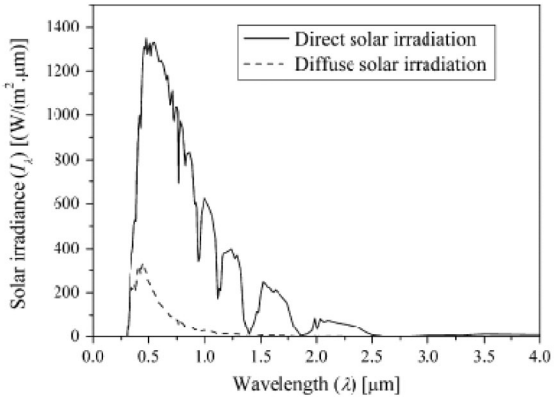

(a)

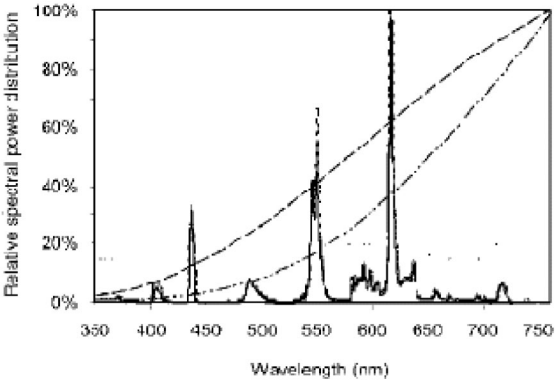

(b)

Figure 2. (a) Direct (solid curve) and diffuse (dashed curve) solar radiation at noon on July 16 at 42°58′ N and 144°22′E [12], and (b) spectral outputs of typical commercial incandescent (dashed curves) and fluorescent (solid curves) lamps at 100% and 30% outputs [13].

differences among the spectral irradiance of sunlight, a commercial fluorescent lamp, and a commercial incandescent light source. Such differences can readily yield variations in the perceived assessment of paper optical properties.

Standard testing methods

In principle, light impinging on a sheet of paper may be reflected from, absorbed by, or transmitted through the sheet. The relative magnitude of each of these three components of the incident light depends not only on the paper characteristics themselves, but also on the illumination characteristics, such as the emission spectrum of the light source, illumination and detection geometry, and backing material. Therefore, several standard methods have been developed to provide guidelines for the testing of optical properties of pulp and paper products. It is evident that the reported values for opacity, gloss, brightness, whiteness and other optical properties of paper are meaningful only in the context of the standard method used for the particular measurement. Table 1 provides a list of such standard methods. A comprehensive discussion on these methods can be found elsewhere [7, 8].

Table 1. ISO and TAPPI standard methods for optical properties of paper.

Property	*Standard Method*	*Property*	*Standard Method*
Opacity	CPPA E.2	Brightness	CPPA E.1
	ISO 2471		ISO 2470
	TAPPI T 425		TAPPI T 452 (45°/0°)
	TAPPI T 519		TAPPI T 525 (d/0°)
Specular Gloss	CPPA E.3	Whiteness	CPPA E.5
	ISO/DIS 8254–1 (75°)		ISO 11475 (D65/10°)
	TAPPI T 480 (75°)		TAPPI T 560 (d/0°)
	TAPPI T 653 (20°)		TAPPI T 562 (45°/0°)
Color	CPPA E.5		
	ISO 5631 (D50/2°)		
	TAPPI T 527 (d/0°)		
	TAPPI T 524 (45°/0°)		

Other laboratory methods

In addition to conventional testing methods, there has been a surge of new laboratory techniques to investigate the optical properties of paper. This trend is mostly driven by rapid advances in computing technology, access to more affordable high-quality digital imaging, and the availability of laser light sources. In particular, characterization of light-paper interactions based on charged couple devices (CCD) has become increasingly popular. These imaging techniques allow for the high-resolution examination of optical

properties of paper and their variations at a microscale level. Several researchers reported using CCD imaging to capture the reflected light from the surface of a sample mounted on a cylindrical sample holder [14–16]. This technique is capable of providing angularly resolved information concerning light reflection. Arney *et al.* studied the gloss of prints using this method [16]. Their device, schematically depicted in Figure 3, consisted of a light source collinear with a cylindrical sample holder. The reflected light was detected using a CCD camera. The illumination was *s*-polarized and a second polarizer was used as analyzer in front of the camera. By analyzing the digital images, the bidirectional reflectance distribution function (BRDF) of the sample was obtained. This device was later calibrated to determine absolute reflectance values at different gloss angles, effective optical constants of paper, and subsurface reflections [17]. Using a similar setup, Lindstrand obtained angularly and spatially resolved information about reflectance and apparent surface inclination. This was achieved by capturing images of the sample while rotating the sample holder. In this way, reflectance information was obtained as a function of the inclination angle for any given spot on the sample. Based on this technique Lindstrand introduced a "gloss angle smoothness" parameter that was found to correlate well with the perceived gloss ranking of paper [15].

Variations of the above experimental setups have been used by other researchers where the sample was mounted on a flat backing [18, 19]. Such a configuration is advantageous in that it can provide information regarding gloss variations over larger areas (several square centimetres). However, compared to the previous setup, it does not provide any angularly resolved information unless the illumination and detection angles are adjusted. Digital imaging technology presents interesting new opportunities in optical testing of paper; however, care must be taken to eliminate potential measurement artefacts. The ultimate spatial resolution of such a system depends on the size of the analysis area, the resolution of the camera, and the optical configuration of the setup. With today's CCD technology, however, it is possible to achieve a spatial resolution of about one micron.

In a recent work, Elton and Preston reported the development of an imaging reflectometer [20]. This device uses a polarized laser beam at a fixed angle of incidence (75°) and a photometric imaging detector to examine the forward scattered light within ±10° about the specular direction. This imaging reflectometer uses two laser beams of wavelengths 635 nm and 670 nm to measure reflectance at various polarizations. A reference beam is used to correct for fluctuations in the light source and the equipment is calibrated using a highly polished glass reference. Using this apparatus, the authors reported measurements of the angular distribution of intensity of reflected

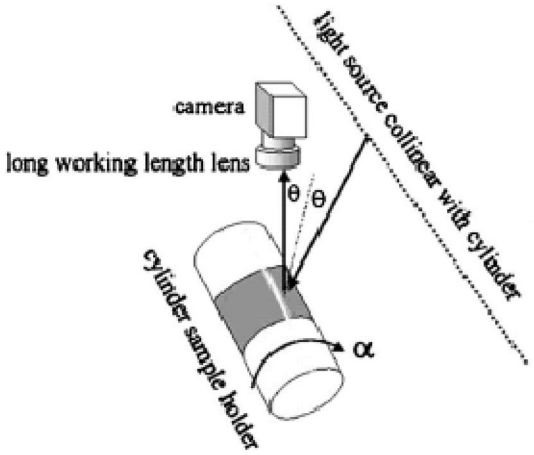

(a)

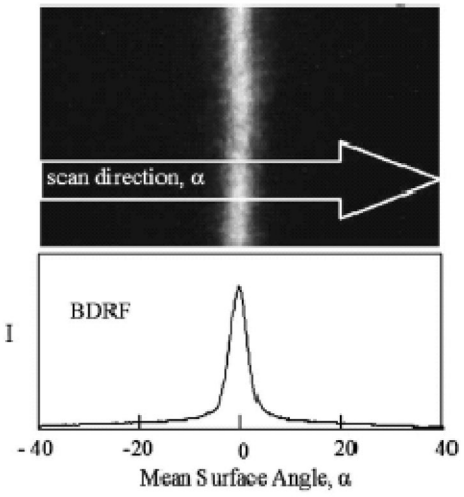

(b)

Figure 3. (a) Imaging micro-goniophotometer, and (b) a typical bidirectional reflectance distribution function. [Scan length is 5 mm [16].]

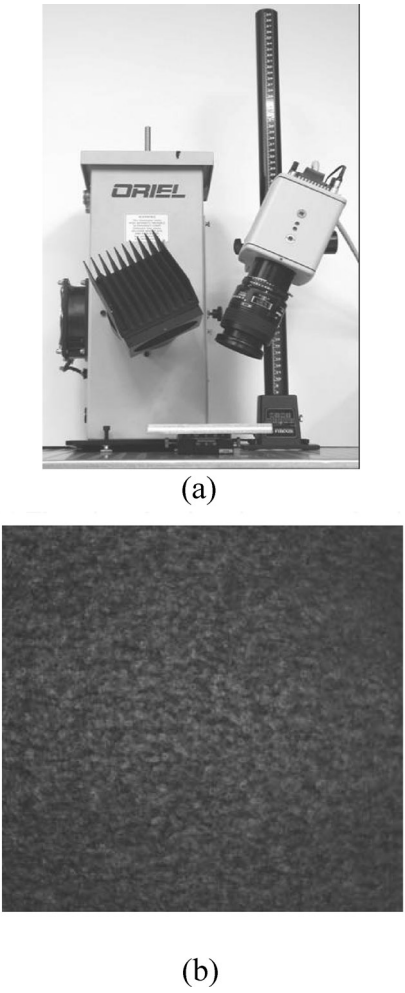

Figure 4. (a) The microgloss imaging set up showing the CCD camera and the ORIEL lamp housing for producing collimated beam of light, and (b) microgloss image of a commercial MWC sample. [The image area is 1.8×1.8 cm [18].]

light (reflectogram) and effective refractive index, as well as optical surface slope distribution and microroughness.

Sung and Keller developed a novel glossmeter based on laser triangulation to obtain simultaneous measurements of local gloss and local roughness of paper [21]. Gloss was determined over regions of about 20×20 μm^2 using a

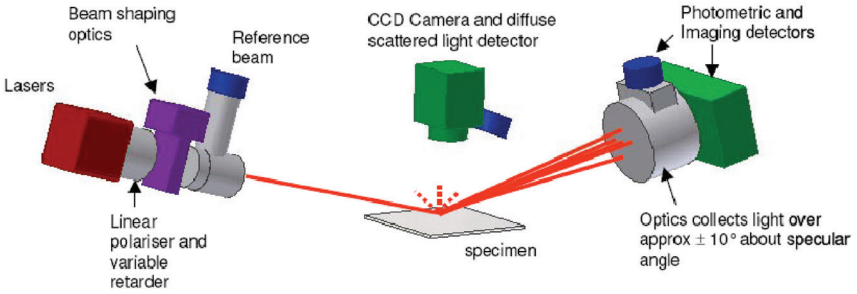

Figure 5. Schematic diagram showing the imaging reflectometer [20].

laser diode (780 nm wavelength) and a CCD array detector. The CCD array had 512 × 64 pixels, providing an imaging range of 150 m. Using this set up, authors measured the local gloss variation, surface topography, and macro-facet map of various commercial paper samples. The measured gloss values were in good agreement with the standard 75° TAPPI gloss values. This device allows for point-by-point examination and correlation between the local gloss map and local macro-facet map of paper samples.

Another method for the analysis of optical properties of paper and prints is based on the use of diffractive optical elements, or DOEs [22–24]. DOEs provide information regarding both the amplitude and the phase of scattered light. In this device, the paper sample is illuminated using a He-Ne laser beam (632.8 nm wavelength). Both reflected and transmitted light is collected and guided through a DOE sensor to form a 4 × 4 light spot on the focal

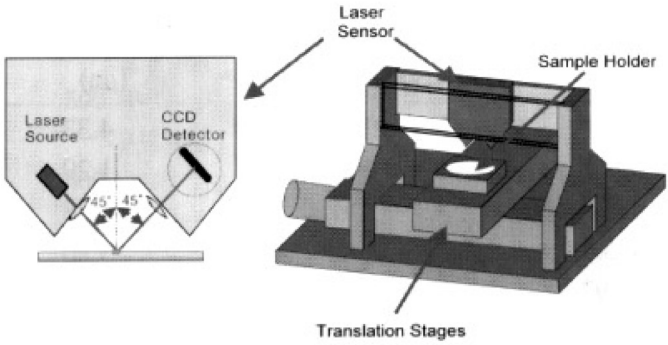

Figure 6. Schematic diagram of laser gloss-roughness measurement device [21].

plane that is captured by a CCD camera. These light spots are typically 30 μm in diameter and are spaced 125 m apart on the focal plane. The difference in the phase of the reflected or transmitted light appears as a speckle pattern that provides information regarding local curvature, defects, and surface anisotropy of paper. This method was recently refined to determine the paper gloss as well as the differential gloss of printed papers [25, 26].

The techniques discussed so far are based on the far field measurements of optical properties of paper. However, Apostol *et al.* argued that the far field measurements of complex particulate media such as paper ". . . depend not only on the bulk heterogeneities (composition and sizes of particulates, for instance) but also on the surface roughness generated by the particles themselves" [27]. In order to decouple these effects, Apostol and co-workers suggested studying the optical phenomena in the proximity of the physical interface using a near-field scattering measurement technique [27, 28]. This device consists of a near field optical microscope with a spatial resolution of 50 nm that allows for simultaneous topographical and optical measurements (Figure 7). The sample is illuminated by a fibre probe with combined propagating and evanescent waves. This probe is positioned at a constant distance and very near the surface (1/50 of wavelength) by the aid of an atomic force microscope. Due to the scattering process, conversion of the evanescent waves into homogeneous waves occurs and is detected by an avalanche photodiode. Using this technique, the authors obtained near-field optical images and the corresponding topography maps of coating layers. In addition, the group developed a discrete random walk model to explain the near-field intensity fluctuations due to local variations in the structure and dielectric properties of the paper coating.

LIGHT REFLECTION AND SCATTERING

Fresnel equations

An analytical model for the reflection of light at the interface of a perfectly smooth dielectric material was first formulated by Augustin Jean Fresnel (1788–1827). Fresnel's equations for the reflectance of s- and p- polarized incident light are given by:

$$R_s = \left(\frac{1 - \varepsilon_r m}{1 + \varepsilon_r m}\right)^2 \tag{1}$$

$$R_p = \left(\frac{1 - \varepsilon_r / m}{1 + \varepsilon_r / m}\right)^2 \tag{2}$$

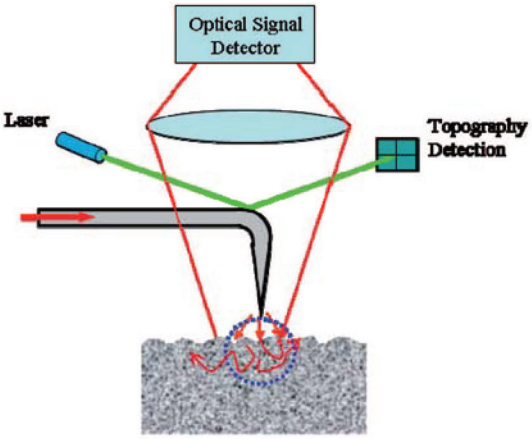

(a)

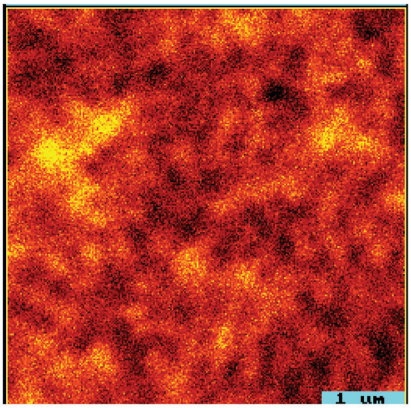

(b)

Figure 7. (a) Near-field scanning optical microscopy system [28], and (b) Near-field intensity distribution of a coating layer containing kaolin and $CaCO_3$ with r.m.s roughness of 22.7 nm [27].

where R_s and R_p are the reflection coefficients for perpendicularly (or s-polarized) and parallel (or p-polarized) light, respectively. ε_r is the ratio of refractive indices (= n_2/n_1), and m is defined as $\cos(\theta_i)$ /$\cos(\theta_t)$ where θ_i and θ_t

are incidence and transmittance angles with respect to the axis normal to the surface. The Fresnel reflectance, R_F, for a non-polarized beam of light can be calculated from:

$$R_F = \frac{1}{2}(R_s + R_p) \tag{3}$$

Based on Fresnel's equations, the intensity of reflected light is only a function of the refractive index of the material and the angle of incidence of light. However, for a complex particulate medium, such as paper, light interaction with randomly distributed particles affects the reflected light intensity and determines its optical properties. Therefore, Fresnel's model is insufficient to describe light reflection from paper thoroughly. However, before addressing this problem, the interaction of light with a single particle will be discussed.

Single particle scattering

Theories dealing with the interaction of light with a single particle can be divided into three categories depending on the particle size, listed below:

1. Particles are much smaller than the wavelength of incident light where Rayleigh-like scattering is dominant. In this case, the scattering cross section of particles increases with the sixth power of particle size. Hence for a given total mass of particles, coarser particles will have a more intense scattering effect.
2. Particles are much larger than the wavelength of incident light and radiation is reflected in specular manner (Fresnel reflection). In this case, the scattering cross section is proportional to particle size to the second power. Hence, for a given total mass, finer particles will have a higher scattering power.
3. Particle size is comparable to the wavelength of light where Mie theory can be applied, depending on the medium density (see below).

Mie theory describes the scattering of a plane electromagnetic wave by an isotropic homogeneous spherical object. Based on this theory, the extinction (τ_t), scattering (τ_s), and absorption (τ_a), cross sections of such a spherical object are given by [29, 30]:

$$\sigma_t = \frac{\lambda^2}{2\pi}\sum_{n=1}^{\infty}(2n+1)\ \mathrm{Re}(a_n + b_n) \tag{4}$$

$$\sigma_s = \frac{\lambda^2}{2\pi}\sum_{n=1}^{\infty}(2n+1)(|a_n|^2 + |b_n|^2) \tag{5}$$

$$\sigma_a = \sigma_t - \sigma_s \tag{6}$$

where a_n and b_n are complex functions of particle size, the refractive indices of the particles and of the medium, and the wavelength of incident light. The scattering (absorption) cross-section is the ratio of scattered (absorbed) power divided by the incident power.

Mie theory has been developed for single particle scattering; however, it is also applicable to random particulate systems with low particle volume concentrations (optical path < 0.1) where single particle scattering dominates. For dense particle systems, an analytical modification of this theory has been recently proposed by Flesia and Schwendimann [31].

In a typical papermaking furnish, the size of filler and pigment particles is of the order of the wavelength of light; hence, Mie theory may be applied. In contrast, fibre dimensions are significantly larger than the wavelength of visible light; however, the surface texture of fibres and the surface fibrillation effects due to refining action may complicate the interaction of light with individual fibres.

Light propagation in random particulate media

Paper may be considered as a random assembly of individual particles, namely fibres and pigments. Propagation of light through a random medium is a complex phenomenon. However, in the case of random media with a low particle concentration, double and multiple scattering events may be ignored, and light scattering can be regarded as single scattering by a particle. Hence, single particle scattering theories may be applied to analyze such systems. As will be discussed later, such an approach has been used to estimate the scattering coefficients of paper coatings.

At high concentrations of particles, multiple scattering is no longer negligible. Theoretical treatments of light propagation in dense media can be classified into two categories: transport (or radiative transfer) theories and multiple wave scattering (or analytical) theories. Transport theories are based on the transport and conservation of energy through a particulate medium while wave scattering theories are based on Maxwell's wave equations. In the following section, a brief introduction to these theoretical treatments is presented.

Radiative transfer equation

The radiative transfer equation (RTE) has been widely used in models for marine biology, underwater visibility, photographic emulsions, and propagation of radiant energy in the atmospheres of planets and stars, as well as optical properties of materials such as papers and coatings. In contrast to wave scattering theories, this theory is approximate and heuristic in the sense that it is not based on a rigorous mathematical foundation. Radiative transfer theory deals with the addition and conservation of power. A general formulation of RTE may be expressed as [29]

$$\frac{dI(\mathbf{r},\hat{\mathbf{s}})}{ds} = -n_p\sigma_t\, I(\mathbf{r},\hat{\mathbf{s}}) + \frac{n_p\sigma_t}{4\pi}\int_{4\pi} p(\hat{\mathbf{s}},\hat{\mathbf{s}}')\, I(\mathbf{r},\hat{\mathbf{s}}')\, d\omega' + \varepsilon(\mathbf{r},\hat{\mathbf{s}}) \qquad (7)$$

Equation (7) is known as the "equation of transfer". Here, I (**r**, **ŝ**) represents the average power flux density at location **r** in the direction **ŝ** within a unit frequency band centred at frequency u over a unit solid angle, n_p is the number of scattering particles in the unit volume, p (**ŝ**, **ŝ′**) is related to the incident power in the direction **ŝ′** that is scattered in the direction **ŝ**, and ε(**r**, **ŝ**) represents the source term.

Unfortunately, there is no known general solution for the radiative transfer equation. However, several useful approximate solutions have been developed for RTE including two-flux models or Kubelka-Munk (KM) theory and the diffusion approximation. These methods will be discussed in subsequent sections.

Light scattering from rough random surfaces

Light scattering from rough surfaces is of interest in many applications including remote sensing, medicine, and materials testing, to name a few. Numerous analytical formulations have been proposed in the literature to examine this problem [29, 32–35]. These models may be classified based on the degree of surface roughness. In surface scattering, the degree of surface roughness depends on the wavelength and direction of incident light as well as surface topography. The criterion that is used to distinguish a smooth surface from a rough one is expressed in terms of the Rayleigh parameter:

$$g_R = 16\,\pi^2\sigma^2\frac{\cos^2\theta_i}{\lambda^2} \qquad (8)$$

Here, σ is root-mean-squared (rms) roughness, θ_i is the angle of incidence,

and λ is the wavelength of incident light. A surface is considered smooth if $g_R \ll 1$ and rough if $g_R \gg 1$.

The two most widely used approaches for the analysis of light scattering by random rough surfaces are the small perturbation method (SPM) and Kirchhoff approximation (KA). The small perturbation method or Bragg theory is based on approximating the scattering amplitude using a Taylor-Volterra expansion of surface heights. In contrast, the Kirchhoff approximation considers a rough surface to behave optically similar to an infinite plane tangent to the surface at the point of interest, such that Fresnel equations can be locally applied.

The Kirchhoff approximation is the oldest and most widely used approximate method. This method is also known as tangent plane approximation (TPA) and the physical optics theory. Strictly speaking, KA is valid for locally smooth surfaces with large local radii of curvature and negligible multiple scattering and shadowing effects. In the high frequency regime, this method reduces to the geometrical optics (GO) or ray optics approximation. The simplest and perhaps most popular form of Kirchhoff approximation considers scattering of a plane, monochromatic, scalar wave by a rough surface with invariant dielectric properties. This method, which is called scalar Kirchhoff theory, is often further simplified by assuming isotropic random surfaces with known statistics, leading to analytical expressions for the coherent (specular) and incoherent (diffuse) field intensities, I_c and I_d. In the case of a Gaussian surface with a Gaussian correlation function, it can be shown that the overall scattered intensity is given by [32]:

$$I_s = I_c + I_d \tag{9}$$

$$I_c = I_o \exp\left(-\frac{g}{2}\right) \tag{10}$$

$$I_d = \frac{k^2 F^2 {L_c}^2 A}{4\pi r^2} \exp(-g) \sum_{n=1}^{\infty} \frac{g^n}{n!\, n} \exp\left(-\frac{k^2 (A^2 + B^2) {L_c}^2}{4\, n}\right) \tag{11}$$

where:

$$g = k^2 \sigma^2 (\cos\theta_i + \cos\theta_s)^2 \tag{12}$$

Here, I_o is the intensity of the coherent field scattered from a smooth surface with the same dimensions, k is the incident wavenumber (= $2\pi/\lambda$), L_c is the

correlation length, A and B depend on the angles of incidence and scattering, and F is an angular factor that depends on the boundary conditions [32].

In addition to the above approaches, a number of unifying schemes have been proposed in an attempt to combine KA and SPM. An example of such a theory is the small slope approximation (or SSA) developed for surfaces with small roughness slopes [36]. Figure 8 provides an overview of the domain of validity of these methods in terms of dimensionless roughness and correlation length. A critical review of these methods can be found elsewhere [37, 38].

In addition to the above approximate methods, a wide range of rigorous numerical solutions has been proposed for scattering from random surfaces. A review of these methods can be found in [39].

In recent years, the Kirchhoff approximation has been used by several researchers to examine the optical properties of paper [40, 41]. This topic will be discussed in more detail in later sections.

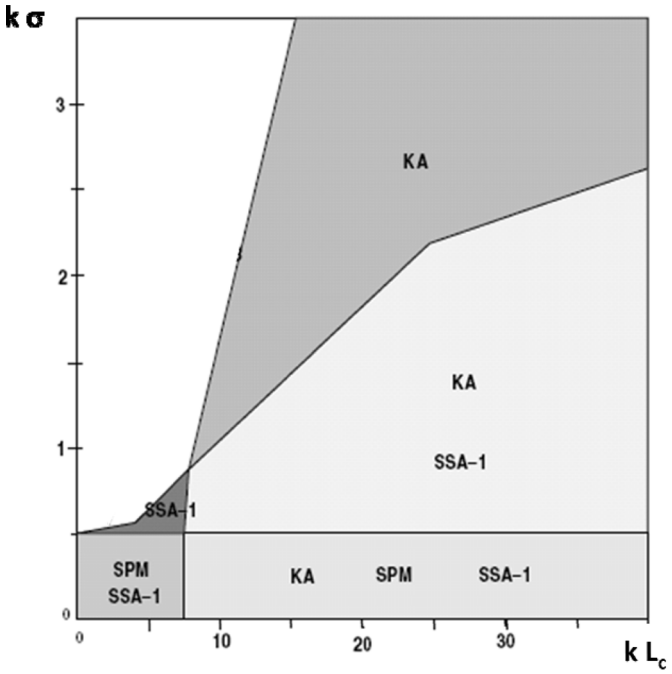

Figure 8. The validity domain of various approximate solution methods for scattering of light from rough random surfaces: $k\sigma$ vs. kLc where k is the wavenumber [38].

KUBELKA-MUNK THEORY

The Kubelka-Munk theory is a two-flux simplification of the radiative transfer model. It is based on treating a turbid random medium, such as paper, as a continuum in the sense that the size of optical inhomogenities is considered small compared to the thickness of the medium. Attenuation of light in this medium is represented by two fluxes propagating in opposite directions, i.e. a forward scattering flux and a backward scattering flux, that are estimated using absorption and scattering coefficients, K and S. This theory provides good predictions for diffuse illumination of dull materials that intensely scatter light. KM theory is not suitable for collimated illuminations and it underestimates the transmittance by several percent if $K/S > 0.01$ [29, 42]. In such cases, a multi-flux model would provide a better prediction of the optical properties of the medium. A rigorous derivation of KM theory can be found elsewhere [43]. In this section, several key results of this model with respect to the optical properties of paper are presented.

Using KM theory, it can be shown that the reflectance of an opaque pile of homogeneous sheet of paper, R_∞, is given by [43]:

$$R_\infty = 1 + \frac{K}{S} - \sqrt{\left(\frac{K}{S}\right)^2 + \frac{2K}{S}} \tag{13}$$

For a single sheet of paper with grammage W, the reflectance of the sheet backed by a non-reflective black cavity, R_o, and the transmittance, T, are obtained from:

$$R_o = \frac{R_\infty \, exp\left(S\,W\,\left(\frac{1}{R_\infty} - R_\infty\right)\right) - R_\infty}{exp\left(S\,W\,\left(\frac{1}{R_\infty} - R_\infty\right)\right) - {R_\infty}^2} \tag{14}$$

$$T = \frac{1 - {R_\infty}^2}{\exp\left(\left(\frac{1}{R_\infty} - R_\infty\right) S\,W\right) - {R_\infty}^2} \tag{15}$$

The above equations are applicable to a single homogeneous layer. However, they may be extended to multi-layer materials such as coated papers. For a two-layer structure (e.g. coated paper), where layer 1 (i.e. the coating layer) is

backed by layer 2 (i.e. base paper), the reflectance and transmittance, $R_{o,12}$ and T_{12}, may be estimated from [8]:

$$R_{o,12} = R_{0,1} + \frac{T_1^2 R_{o,2}}{1 - R_{o,1}R_{o,2}} \tag{16}$$

$$T_{12} = \frac{T_1 T_2}{1 - R_{o,1}R_{o,2}} \tag{17}$$

Here, subscripts 1 and 2 refer to layers 1 and 2, respectively.

In the case of a large enough pile of such a two-layer material, the reflectance, $R_{\infty,12}$, can be estimated from:

$$R_{\infty,12} = \frac{1 + R_{o,12}^2 - T_{12}^2}{2R_{o,12}} - \sqrt{\left(\frac{1 + R_{o,12}^2 - T_{12}^2}{2R_{o,12}}\right)^2 - 1} \tag{18}$$

Absorption and scattering cross sections

It has been shown that K and S are related to radiative transfer theory's scattering and absorption cross sections, i.e. σ_s and σ_a. In their simplest forms, these relationships may be expressed by [44]:

$$K = 2\,\sigma_a \tag{19}$$

$$S = \frac{3}{4}\,\sigma_s' \tag{20}$$

In this equation, $\sigma_s' = \sigma\,(1 - g)$, where g is the asymmetry factor. This factor is the average cosine of the scattering angle that can be determined from:

$$g = \int_0^{\pi} p(\theta)\cos(\theta)\,d\theta \tag{21}$$

$p(\theta)$ is the distribution of the scattering angle, also known as the phase function.

Several other models have been proposed in the literature, leading to expressions similar to those of KM theory. In particular, Silvy used a

corpuscular approach to study the interaction of light with non-homogeneous non-emitting dense media that absorb much less light than they scatter. By applying statistical laws for scattering and absorption (represented by elastic and inelastic collisions) and using the diffusion approximation, he arrived at an equation similar to KM theory with the absorption and scattering cross sections are given by [45, 46]:

$$K = 2\,\sigma_a \tag{22}$$

$$S = \frac{3}{4}\,\sigma_s - \sigma_a \tag{23}$$

Mudgett and Richards compared the predictions of KM theory with those of a many-flux solution to RTE and obtained empirical expressions for the scattering and absorption of the medium [42]:

$$S \cong \frac{1}{4}(3\,a_o - a_1)\,\sigma_s \tag{24}$$

where a_o and a_1 are Legendre polynomial coefficients of the phase function. In a more recent study, Jacques proposed a semi-empirical model for the reflectance of a semi-infinite medium based on the diffusion theory of light [47]. This model, similar to the Beer-Lambert law, is expressed by:

$$R_\infty = \exp(-C_o\,\sigma_a\,\delta) \tag{25}$$

where R_∞ is the total diffuse reflectance, C_o is a constant, and δ is the penetration depth that depends on the transport scattering and absorption cross sections, i.e. σ_s and σ_a, and is given by:

$$\delta = [3\,\sigma_a\,(\sigma_a + \sigma_s')\,]^{-1/2} \tag{26}$$

By comparing Equation (26) with the numerical solution of RTE, Thennadil showed that Equation (25) is accurate with better than 1% error for $\sigma_a/\sigma_s' < 0.1$ [48]. He also found that for diffuse illumination, $C_o = 4.0$, while for collimated illumination, C_o is dependent on the anisotropy factor and may be empirically described as a second order polynomial:

$$C_o = f(g) = 4.8446 + 0.472\,g - 0.114\,g^2 \tag{27}$$

The transport scattering and absorption cross sections in Thennadil's

equation are related to the absorption and scattering coefficients of KM theory according to:

$$K = 2\,\sigma_a \tag{28}$$

$$S = \frac{12}{C_o^2}\,\sigma_s' \tag{29}$$

A comparison between predictions from the solution to RTE and those of KM theory based on Thennadil's model for collimated illumination is shown in Figure 9. For comparison, results of KM theory for diffuse illumination (C_o = 4.0) are also plotted in Figure 9.

There are several other theoretical models that relate RTE cross sections to the KM absorption and scattering coefficients. These results may be expressed by the following general equations:

$$K = 2\,\sigma_a \tag{30}$$

$$S = m_1\,\sigma_s' - m_2\,\sigma_a \tag{31}$$

where m_1 and m_2 are constants given in Table 2.

Table 2. Values for parameters m_1 and m_2 in Equation (31).

m_1	m_2	*Ref.*
$\frac{3}{4}$	1	[46], [49]
$\frac{3}{4}$	0	[44]
$\frac{3}{4}$	$\frac{1}{4}$	[50]
$\frac{12}{C_o^2}$	0	[48]

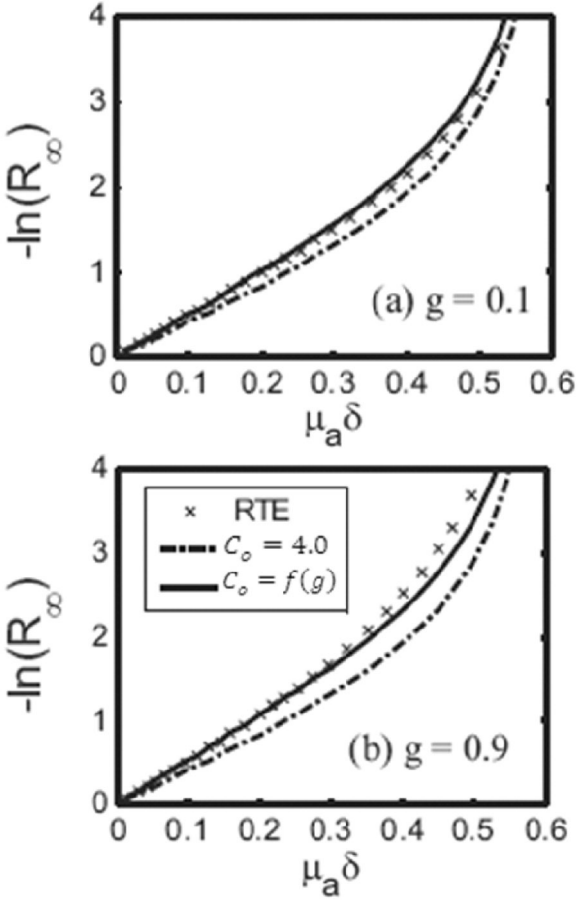

Figure 9. Comparison between RTE solution (x) for collimated illumination and KM prediction using Thennadil's model for two values of g. Solid curve: C_o is given by equation (27), dashed curve: $C_o = 4.0$ [48].

Factors affecting K and S

Absorption and scattering coefficients of paper depend on furnish and papermaking operations, such as fibre type, pulping, bleaching, beating, wet pressing, and calendering, and on filler and pigment type and amount [9]. In practice, the values of K and S are estimated from diffuse reflectance measurements. The scattering coefficient is related to the specific surface area

and pore structure of the scattering medium. In studying thermomechanical pulp (TMP) handsheets containing a variety of fines and fillers, Alince *et al.* found a poor correlation between the specific light scattering coefficient and the total porosity or the total surface area as estimated by mercury intrusion porosimetry [51]. In contrast, the authors observed a good correlation when pores smaller than 100 nm were excluded from the measurement, and hence suggested that the pore structure smaller than this threshold does not contribute to light scattering. However, by comparing Brunauer-Emmett-Teller (BET) adsorption analysis and mercury intrusion porosimetry measurement, Lehtonen and Dyer suggested that the concept of optically active pores could be a measurement artefact caused by the destruction of paper's pore structure during mercury intrusion porosimetry [52].

Theoretically, K and S are expected to be independent parameters; however, it has long been known that S decreases for a highly absorbing medium. Foote found the scattering coefficient of a dyed sample with a reflectance of 0.10 was two-thirds of that of an identical but undyed sample with a reflectance of 0.71 [53]. Later, it was shown that the reduction of the scattering coefficient spans over the absorption spectrum of the dyestuff [54]. This effect was also observed by varying the amount of fines in mechanical pulp handsheets [52]. To rationalize this anomaly, known as the "Foote effect", two possible explanations have been suggested in the literature: firstly, that dye addition changes optical properties of the cell wall; i.e. the surface reflectance of and internal absorption [55]; and secondly, that this anomaly is caused by an inherent error in the KM theory [56].

For mechanical pulp-based papers, where the absorption coefficient may affect the scattering coefficient and the pore structure can be quite variable, the relationship between the specific surface area and scattering coefficient is not trivial. In this case, however, it was found that the scattering coefficient is a measure of specific surface area as long as the wavelength of light used in measuring the scattering is outside the range of the "Foote effect" [52].

In addition to the above consideration, it is important to note that measurements of K and S are based on reflectance measurements that may be affected by both surface and bulk scattering effects. In fact, Granberg and coworkers found that the estimated absorption and scattering coefficients are not only dependent on the sheet structure but also can be significantly affected by nonuniformity in surface reflectance due to surface topography effects [57].

Over the years, several extensions for the KM theory have been proposed to improve its domain of applicability [58, 59]. Despite these attempts, a key issue concerning the KM theory remains: the absorption and scattering coefficients, K and S, are merely model parameters that do not represent intrinsic

properties of the material [60]. However, KM theory remains as one of the most widely used theories for the interaction of light with paper and coatings, thanks to its simplicity. A detailed discussion on the applications and modifications of KM theory can be found elsewhere [61].

OPTICAL PROPERTIES

As discussed earlier, the perceived value of paper products depends on their appearance. Words such as whiteness, brightness, opacity, and gloss are often used to describe the visual perception of paper. From a practical point of view it is important to quantify these "optical properties" by means of reliable and repeatable measurement methods, and furthermore, to relate these measured values to furnish characteristics and paper structure. In what follows, some of the recent advances in our fundamental understanding of the aforementioned optical properties of paper will be presented.

Whiteness

Ganz described whiteness as "an attribute of colors of high luminous reflectance and low purity situated in a relatively narrow region of the color space along dominant wavelengths of 570 nm and 470 nm approximately" [62]. Whiteness is a colorimetric parameter that can be influenced by the lighting conditions. According to CIE, whiteness can be quantified based on the tristimulus values [63]:

$$Whiteness = Y + 800\ (x_n - x) + 1700(y_n - y) \tag{32}$$

Similarly, tint is defined as:

$$Tint = 1000(x_n - x) - 650(y_n - y) \tag{33}$$

Here x_n and y_n depend on the choice of illuminant, and x and y are functions of the tristimulus values, i.e. X, Y, and Z, where:

$$x = \frac{X}{X + Y + Z} \tag{34}$$

$$y = \frac{Y}{X + Y + Z} \tag{35}$$

Under D65/10° illumination, a specimen is to be considered white if $40 < W_{10} < (5\ Y_{10} - 280)$ and $-3 < T_{W,10} < 3$. This definition of whiteness correlates well with the visual ranking tests and it is easy to interpret. However, the choice of illuminant is an important consideration in the measurement of whiteness. According to ISO, there are two standards for the illuminant: D65, that is suitable for daylight, and illuminant *C* that is applicable to the indoor conditions. The main difference between these two illuminants is the UV component of the emission.

Whiteness of a near white object is affected by the so-called "lightness" but is not equal to it. In studying the whiteness of 35 commercial office papers, Bonham found that changes in the brightness alone explained much of the variability in the whiteness with the lightness (L^*) being responsible for the residual error and the scattering of data [64]. He found that whiteness could be expressed by a linear combination of lightness and reflectance factor, $R_z = Z/Z_n$:

$$W = 340 - 5.56\,L^* + 3.14\,R_z \tag{36}$$

Traditionally, whiteness of paper has been controlled by bleaching and bluing the substrate and the addition of purifying pigments [62]. Based on the definition of whiteness, a bluish shade has a positive effect on whiteness and tint. Therefore, by introducing blue dyes to the papermaking furnish, one could adjust the whiteness and tint of paper products [65–67]. Liu *et al.* reported that the yellow tint of high yield pulp could be minimized or eliminated by the addition of a suitable dye. They also found that with the addition of about 4 ppm dye (based on pulp), the CIE whiteness and lightness of the pulp reached those of market kraft pulp [65]. The addition of dye to the coating formulation has also proved to be an effective method to adjust the whiteness of coated papers. Table 3 shows the effect of addition of a blue dye on the CIE whiteness and tristimulus values of a coated paper. This result shows

Table 3. Brightness, CIE whiteness and tristimulus values for various levels of addition of a blue dye to the coating formulation in terms of % in dry dye weight [68].

Dye %	*CIE Whiteness*	*Tappi Brightness*	*X*	*Y*	*Z*
0	44	71	71	74	72
0.25	58	68	67	69	72
0.50	71	66	62	64	70

that whiteness continuously increases while brightness decreases with the addition of a blue dye [68].

Improving optical properties of uncoated paper by dye addition has been the subject of several recent theoretical studies. Dye addition forms color by subtraction, i.e. by absorbing and reducing/eliminating certain wavelengths from the light. Using KM theory, Mäkinen and co-workers studied the effect of dye addition on whiteness of uncoated papers. Assuming a Gaussian absorption model for the dye, the total absorption coefficient of dyed paper, K, was calculated as below [69]:

$$K = K_p + K_d \tag{37}$$

$$K_d = A\, exp\left(-\frac{(\lambda - \lambda_c)^2}{\beta^2}\right) \tag{38}$$

where K_p, and K_d are absorption coefficients of paper and dye, respectively, λ is the wavelength of light, λ_c is the wavelength of maximum absorption of the dye, and β is half peak absorption of the dye. Hence, the tristimulus value, X_{10}, was calculated from:

$$X_{10} = \int E(\lambda)\, R(\lambda)\, \bar{x}_{10}(\lambda).\, d\lambda \tag{39}$$

Similar equations can be written for Y_{10} and Z_{10} simply by replacing X_{10} with Y_{10} or Z_{10}, and $\bar{x}_{10}$ with $\bar{y}_{10}$ or $\bar{z}_{10}$, where $\bar{x}_{10}$, $\bar{y}_{10}$, and $\bar{z}_{10}$ are the CIE color matching functions. Hence, whiteness can be calculated from Equation (32) (see Figure 10). Based on this approach, Mäkinen *et al.* concluded that the required amount blue dye for a modest gain in whiteness is a function of the dye distribution; however, the maximum achievable increase in whiteness is independent of the dye distribution.

Since whiteness is determined by measuring the reflection of light from paper, the surface structure of paper is expected to influence the perceived whiteness values. Makarenko and Shaykevich studied this effect by the numerical modeling of the scattering of light from a specimen under standard illumination geometries [70]. They suggested that the resultant intensity of the light scattered by the specimen I_r may be approximated by adding the intensities of the volume scattering I_v and the surface scattering, I_s, of the specimen. Therefore, the relative spectral scattering coefficient of the specimen at wavelength λ, i.e. $R(\lambda)$, may be calculated from:

$$R(\lambda) = \frac{I_r(\lambda)}{I_o(\lambda)} = \frac{I_v(\lambda)}{I_o(\lambda)} + \frac{I_s(\lambda)}{I_o(\lambda)} \tag{40}$$

In this equation, I_o is the intensity of scattered light from a reference specimen. To estimate the volume scattering, authors considered scattering from an infinitely thick layer with spectral photon revival probability represented by Λ. Assuming a uniform angular distribution of scattered light, the index of scattering in direction γ can be estimated based on:

$$\rho(\eta, \xi) = \frac{\Lambda}{4} \frac{\varphi(\eta)\, \varphi(\xi)}{\eta + \xi} \tag{41}$$

In this equation η, and ξ are the cosines of angles of observation and incidence of light, and φ is an auxiliary function that characterizes the intensity of luminous flux near the surface:

$$\varphi(\eta) = \frac{1 + 2\,\eta}{1 + 2\,\eta\sqrt{1 - \Lambda}} \tag{42}$$

The relationships for non-spherical scattering indicatrix are more complicated; more detail on this subject may be found in [70]. To account for surface scattering, the authors considered surfaces with irregularities at the scale of

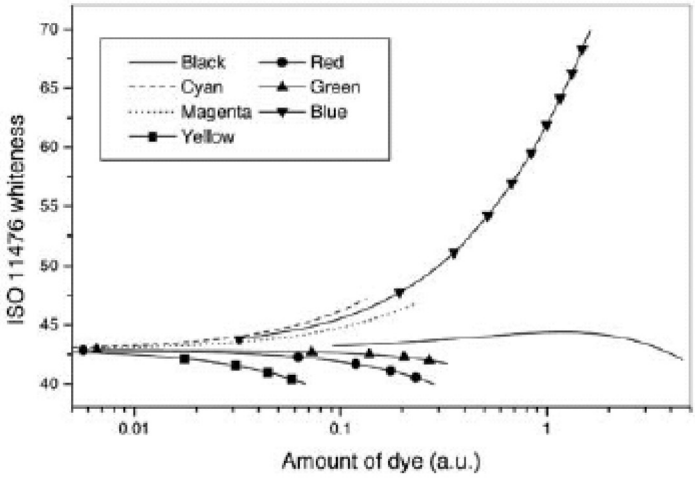

Figure 10. Effect of dye addition on ISO whiteness based on KM theory [69].

the incident light wavelength to be either a) small and gently sloped, or; b) smooth. Small and gentle irregularities mean that the root-mean-square surface height is much smaller than both the wavelength of light and the size of surface irregularities, i.e. the correlation length L_c. In this case, the scattering cross section can be estimated from Bass and Fuks formulae:

$$\sigma_s = \frac{R_F}{4\pi}\frac{{L_c}^2}{\sigma^2}\left\{\left[\frac{\cos\varphi\cos\chi - \cos\psi\ (1+\sin\varphi\sin\chi)}{(\sin\varphi+\sin\chi)^2}\right] + \frac{sin^2\psi}{(\sin\varphi+\sin\chi)^2}\right\}\times \exp\left\{-\left(\frac{L_c}{2\sigma}\right)^2\frac{cos^2\varphi + cos^2\chi - 2\cos\psi\cos\varphi\cos\chi}{(\sin\varphi+\sin\chi)^2}\right\} \tag{43}$$

For smooth surfaces (case b), Beckman-Spizzichino's model may be used:

$$\sigma_s = R_F \exp\left(-\frac{16\,\pi^2\sigma^2 sin^2\varphi}{\lambda^2}\right) \tag{44}$$

Here, R_F is the Fresnel reflectance, and the angles φ, χ, and ψ are defined in Figure 11.

Using the above equations, the intensity of reflected light from the sample was determined by integrating the scattered flux over both the specimen and the surface of the integrating sphere (Figure 11). This calculation was repeated for the reference material and the relative spectral scattering coefficient of the specimen at wavelength λ, i.e. $R(\lambda)$, was obtained from Equation (40). Based on this approach, the effects of surface roughness on the tristimulus coordinate Y_{10}, whiteness and tint of weakly absorbing papers with high volume scattering were predicted.

Figure 12 shows the results of this study under three measurement conditions: 1) ISO illumination with only diffuse reflectance detected, 2) ISO illumination with diffuse reflectance and some specular reflection detected, and 3) illuminant modeled as a cloudy sky. It was found that whiteness and tint were dependent both on the measurement/illumination conditions and on the surface roughness. However, the effect of roughness on whiteness was detectable only when the specular reflectance was also taken into account. In contrast, the chromaticity coordinates of paper were found to be independent of both roughness and the measurement scheme.

As discussed before, a bluish shade increases the measured value of whiteness. This fact has been exploited by papermakers in the recent years through the addition of optical brightening agents (OBA) in the production of various grades of papers to enhance brightness and whiteness [71]. Optical

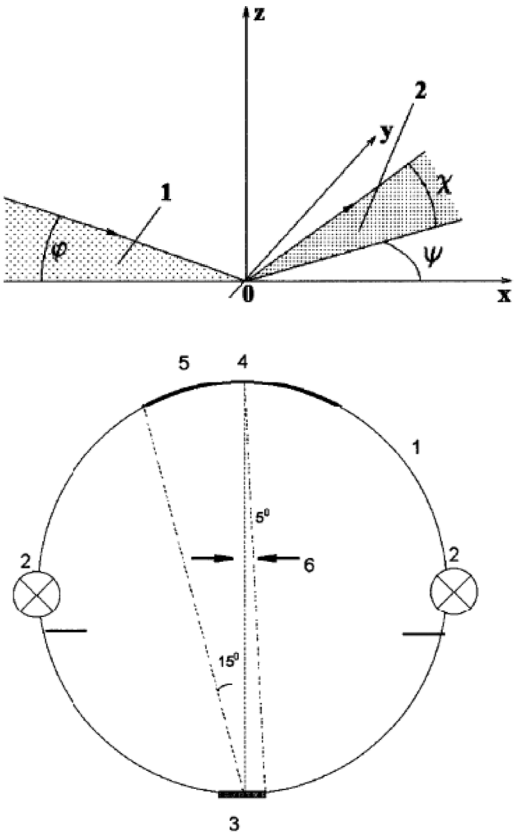

Figure 11. Top: angles φ, χ, and ψ in equations(43) and (44). 1 and 2 are planes of incident and scattering; bottom: reflectometer geometry showing 1- integrating sphere, 2- light source, 3- specimen, 4- point of observation, 5- black ring, and 6- glossy trap [70].

brightening agents or fluorescent whitening agents (FWA) can shade the yellow tint of paper and improve the whiteness of the product. Optical whiteners function by absorbing ultraviolet radiation and re-emitting blue light. A comparison of various types of OBAs that are currently used in the paper industry can be found elsewhere [72]. The addition of OBAs is particularly of interest since there is an increasing trend towards using mechanical pulps in traditionally wood-free grades. Liu *et al.* reported that by the addition of OBAs, the CIE whiteness of laboratory handsheets made of high yield pulp was significantly enhanced; however, OBA addition was less cost effective

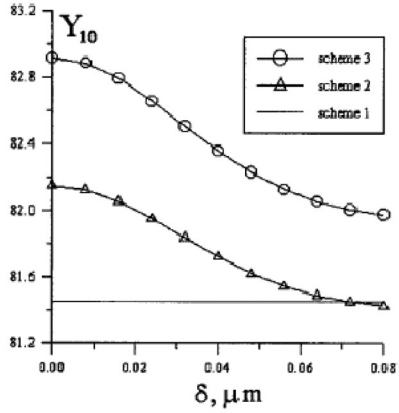
Y_{10}
scheme 3
scheme 2
scheme 1
δ, μm

(a)

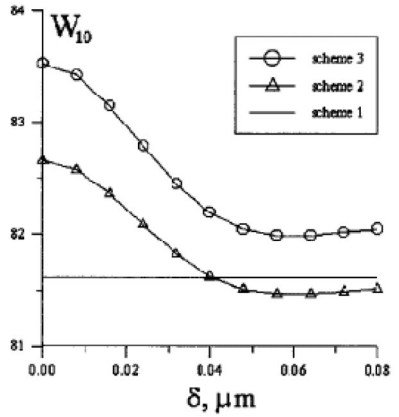
W_{10}
scheme 3
scheme 2
scheme 1
δ, μm

(b)

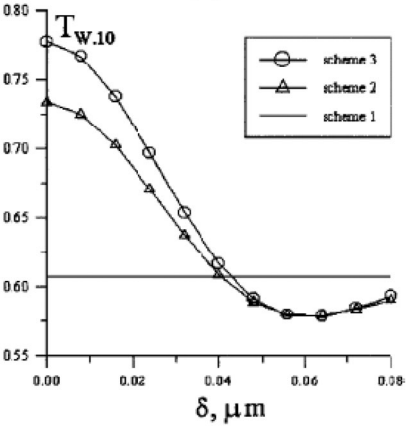
$T_{w.10}$
scheme 3
scheme 2
scheme 1
δ, μm

(c)

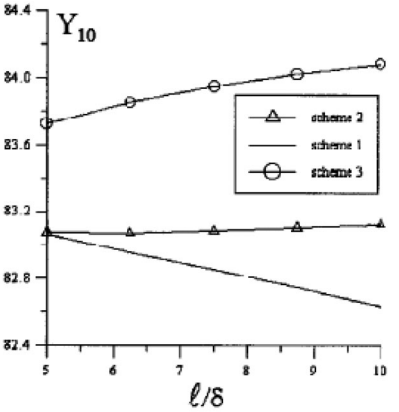
Y_{10}
scheme 2
scheme 1
scheme 3
ℓ/δ

(d)

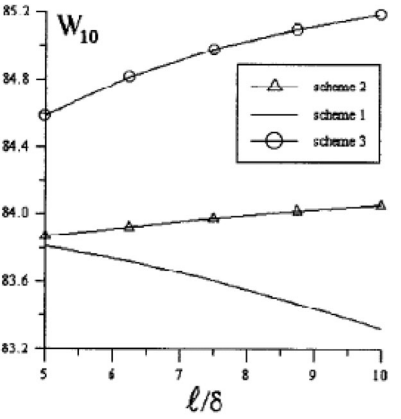
W_{10}
scheme 2
scheme 1
scheme 3
ℓ/δ

(e)

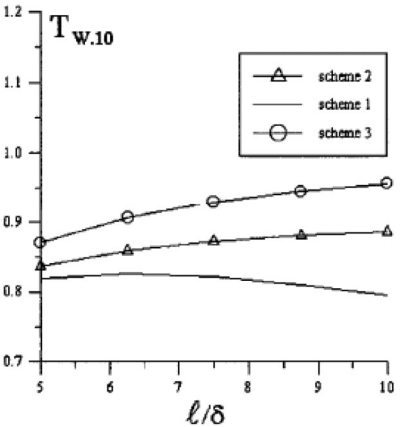
$T_{w.10}$
scheme 2
scheme 1
scheme 3
ℓ/δ

(f)

compared to the addition of dyes in improving whiteness. Furthermore, it has been shown that heat can completely destroy OBAs creating optical mottle [73], and that the optical properties of papers containing OBAs degrade faster than papers without OBA addition both under the influence of light and in dark storage [74]. Beside wet-end applications, OBA could be also added to the coating formulation. One of the key issues in such applications is the compatibility of coating formulations with OBAs. Ma *et al.* investigated the distribution of fluorescent whitening agents in coating layers containing ground calcium carbonate (GCC) and clay [75]. The results of their study suggested that a higher OBA concentration near to the coating surface produced a higher whiteness.

The mathematical models presented so far do not account for the fluorescence effects due to the addition of OBAs. In order to estimate such effects, one may use the modified KM theory proposed by Bonham for colorant formulation of newsprint [76]. According to this model, the reflectance of a thick pile of paper containing a fluorescent dye at a given wavelength, $R_{\infty,OBA}(\lambda)$, may be estimated from:

$$R_{\infty,OBA}(\lambda) = R_{\infty}(\lambda) + (1 + R_{\infty}(\lambda)) \frac{Q(\lambda)}{2\, I_o(\lambda)} F(\lambda) \tag{45}$$

Here, $R_{\infty}(\lambda)$ is the KM reflectance at wavelength λ given by Equation (13), $Q(\lambda)$ is the quantum yield of fluorescent dye per unit wavelength, $I_o(\lambda)$ is the intensity of incident light at wavelength λ, and F is an auxiliary function that is defined as:

$$F(\lambda) = \int_{\lambda_1}^{\lambda_2} \frac{K(\lambda') - K_o(\lambda')}{A(\lambda) - A(\lambda')} \left(1 + R_{\infty}(\lambda')\right) I_o(\lambda').d\lambda' \tag{46}$$

where λ_1 and λ_2 are limits of the absorption band of the dye, $K(\lambda)$ is the absorption coefficient at wavelength λ for paper with OBA, $K_o(\lambda)$ is the absorption coefficient at wavelength λ for paper without OBA, and $A(\lambda)$ is equal to $\sqrt{K^2(\lambda) + 2\ K(\lambda)\ S(\lambda)}$. Bonham used the above model to back-

Figure 12 (opposite). Effect of surface roughness on the tristimulus coordinate, Y_{10}, whiteness, and tint for a smooth (left) and rough (right) surface under three model illumination schemes: 1- ISO illumination with only diffuse reflectance detected, 2- ISO illumination with diffuse and some specular reflectance detected, and 3- illuminant is modeled as cloudy sky [70].

calculate the absorption and emission spectra of the fluorescent dye in a newsprint sample, and applied the results to color prediction. Once the tristimulus color values are determined, one can readily calculate the whiteness value.

Brightness

Brightness is defined as the reflectance of blue light with a spectral distribution peaking at 457 nm compared to that of a perfectly reflecting, perfectly diffusive surface [1]. Brightness has been used for more than sixty years to monitor the pulp bleaching process. The wide application of brightness as a measure of quality is due to three reasons: 1) brightness measurement is simpler than measuring color (which requires 3 values); 2) this measurement is especially sensitive to the blue region of the spectrum where pulp bleaching has its main effect, and; 3) the brightness value is related to the perceived whiteness [5]. There is no strict relationship between brightness and CIE variables; however, brightness values are very similar to the reflectance factor, R_z, defined by [64]:

$$R_z = 100\frac{Z}{Z_n} \tag{47}$$

Here, Z is the tristimulus coordinate, and the value of Z_n depends on the illumination characteristics [63]. Brightness can be also expressed in terms of the CIELAB color coordinates, $L^*a^*b^*$, that are defined as:

$$L^* = 116\,(Y/Y_n)^{1/3} - 16 \tag{48}$$

$$a^* = 500\left[(X/X_n)^{1/3} - (Y/Y_n)^{1/3}\right] \tag{49}$$

$$b^* = 200\left[(Y/Y)^{1/3} - (Z/Z_n)^{1/3}\right] \tag{50}$$

Therefore,

$$R_z = 100\left(\frac{L^* + 16}{116} - \frac{b^*}{200}\right)^3 \tag{51}$$

However, since the measurement of brightness is limited to the blue region of the spectrum, it is not an adequate representation of perceived whiteness as assessed under indoor or outdoor illumination. Furthermore, brightness is not sensitive to papers treated by the deinking process; any ink residues mostly absorb larger wavelengths [5].

Based on its definition, brightness may be estimated from Equation (13) with the scattering and absorption coefficients at 457 nm. However, as pointed out earlier, OBAs are frequently added to pulp and paper products to improve the brightness. In such cases, the modified KM theory has to be used to account for fluorescence effects as in Equation (45).

Paper brightness is affected by bleaching, degree of beating, wet pressing, type and amount of fillers and dye and OBA addition, as well as coating and calendering. Addition of fillers improves the brightness of paper by increasing the scattering coefficient due to increased specific surface area. On the other hand, as discussed earlier, dyes and OBAs improve brightness by imparting a bluish shade to the paper. The pore structure of paper influences the brightness as well, such that higher calendering levels generally cause a reduction in brightness due to the collapse of fibres and pores. In addition, it has been reported that brightness uniformity is adversely affected by poor formation in OBA-containing papers [77].

In the case of coated papers, the coating layer significantly affects the product brightness. Pigment type, average size and size distribution, and shape affect the ability of coated papers to scatter light and hence influence brightness and opacity of the paper. Light scattering efficiency of a coating layer is determined by its pore structure. In studying GCC and precipitated calcium carbonate (PCC) pigments, Hallam and Hiorns demonstrated that the coating scattering coefficient closely followed the Mie theory: light scattering per void increased by increasing the average distance between TiO_2 particles as well as the pore diameter and peaked when the pore size was about 400 to 450 nm [78]. For mechanical pulp containing papers, a coating layer not only improves brightness but also enhances the brightness' stability [79].

Opacity

Opacity is a measure of perceived covering ability of paper. Although this quality of paper is related to its non-transparency (low transmittance), in practice, it is quantified through reflectance measurements.

There are two main standard methods to measure opacity: TAPPI 425 and ISO 2471 (TAPPI 519 is another method similar to ISO 2471), where opacity is defined as:

$$OP_{ISO} = 100\,\frac{R_o}{R_\infty} \tag{52}$$

$$OP_{T425} = 100\,\frac{R_o}{R_{0.89}} \tag{53}$$

Here, R_o is the reflectance of a single sheet of paper backed by a black backing, R_∞ is the reflectance of an opaque pile of paper, and $R_{0.89}$ is the reflectance of a single sheet of paper over a standard backing with a reflectance of 89%. It is important to keep in mind that the ISO standard is determined at diffuse illumination and 0° detection angle, while the TAPPI T425 standard is based on 15°/diffuse geometry. Both methods are based on the human vision model and use the CIE 1931 color matching function, $\bar{y}(\lambda)$.

Opacity may be estimated based on KM coefficients and using Equations (13) to (15) and recognizing that $R_{0.89}$ can be expressed by [80]:

$$R_{0.89} = \frac{R_o - 0.89\,(1/R_\infty + R_\infty)R_o + 0.89}{1 - 0.89\,R_o} \tag{54}$$

The above opacity standards were developed to quantify the degree by which the printed areas appear darker once viewed from the reverse (unprinted) side of a single sheet of paper. By definition, opacity standards are based on lightness (or equivalently tristimulus Y) only. This creates a problem with the perceived opacity of coloured papers [81]. For coloured papers, the black print on the back of paper changes hue and saturation as well as lightness. Therefore, the standard opacity measurements are restricted to white or near white samples [82]. To address this issue, Mäkinen *et al.* proposed the use of the CIE 1994 standard for color difference to quantify the covering ability of papers:

$$\Delta E_{94} = \sqrt{\left(\frac{\Delta \mathrm{L}^*}{\mathrm{k_L S_L}}\right)^2 + \left(\frac{\Delta \mathrm{C}^*}{\mathrm{k_C S_C}}\right)^2 + \left(\frac{\Delta \mathrm{H}^*}{\mathrm{k_H S_H}}\right)^2} \tag{55}$$

where ΔL*, ΔC*, ΔH* are differences in the lightness, chroma, and hue, respectively:

$$\Delta \mathrm{L}^* = L_2^* - L_1^*$$

$$\Delta \mathrm{C}^* = C_2^* - C_1^*$$

$$\Delta \mathrm{H}^* = \sqrt{(a_2^* - a_1^*)^2 + (b_2^* - b_1^*)^2 + (C_2^* - C_1^*)^2}$$

$$S_L = 1\,; \quad S_C = 1 + 0.045\sqrt{C_1^* C_2^*} \quad ; \quad S_H = 1 + 0.015\sqrt{C_1^* C_2^*}$$

Here, C_i^* (i = 1, 2) is the chroma defined as $\sqrt{a_i^* + b_i^*}$, and k_L, k_C, and k_H may be used to correct for deviations from CIE 1994 reference viewing conditions.

Mäkinen *et al.* analyzed the opacity of three sets of printed samples: black

prints on white papers, black prints on color newsprint, and color prints on white paper. They found that the standard opacity; i.e. that described in Equation (52), was unable to predict the hiding ability of coloured papers, while CIE 1994 color difference (Equation (55)) adequately ranked and quantified the perceived opacity of all samples.

Using KM theory presented by Equations (37) to (39), Mäkinen *et al.* studied the effect of dye addition and distribution on paper opacity [69]. They found that it was challenging to achieve both a good opacity and a high whiteness by dye addition. Furthermore, since opacity depends on light transmittance, dye distribution was found to have little or no effect on opacity. However, if paper whiteness was limiting, adding dye to the centre of paper was found to give a higher opacity while maintaining a good level of whiteness.

It is worthwhile to point out that for a rough scattering medium such as paper theoretical analysis has shown that the transmitted light is affected by the surface roughness [83]. Although this effect may not be significant for diffuse illumination measurements, it could play a role in directional opacity tests, i.e. TAPPI T425 15°/diffuse geometry.

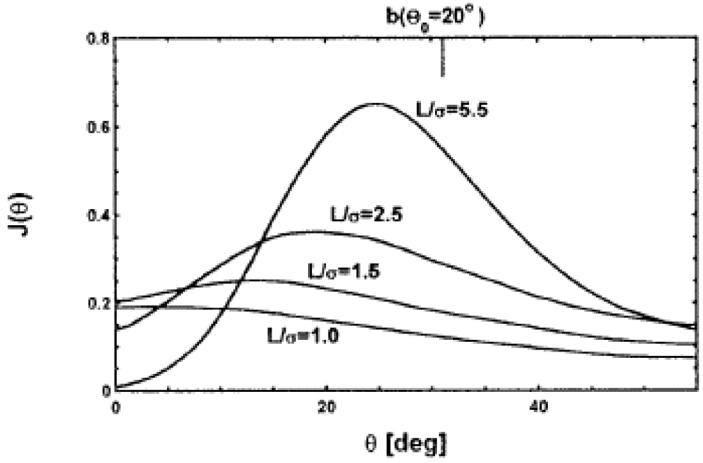

Figure 13. Angular dependence of the transmitted flux through a medium with a refractive index of 1.5 relative to the ambient as a function of L_c/σ. The incident angle is 20° [83].

Specular gloss

Gloss, as previously mentioned, is an attribute of paper that relates to its "shininess". Gloss not only depends on material structure and characteristics but also on measurement geometry and illumination conditions. It is quantified as the ratio of the specular reflection of a sample, $R(\theta)$, to that of a reference material, $R_{ref}(\theta)$:

$$G(\theta) = 100\frac{R(\theta)}{R_{ref}(\theta)} \tag{56}$$

The traditional reference material used for gloss measurements is a polished black glass with refractive index of $n_{ref} = 1.527$. However, recent studies have shown that black glass standards are prone to aging, contamination, and damage. Therefore, a new primary standard has been recently developed by NIST that is a highly pure BaK50 glass with a refractive index of 1.5677 [84].

According to Fresnel's equations, gloss is expected to depend on the angle of incidence and refractive index of the material. For rough materials, however, experimental evidence suggests that gloss is also a function of the surface texture of paper.

By studying high-gloss coating layers applied on smooth films (i.e. $g_R \ll 1$), Gate *et al.* found that gloss could be predicted based on the rms roughness of the coating layer according to the Beckman-Spizzichino relationship [85]:

$$G = G_m \exp(-g_R) \tag{57}$$

where G_m is the maximum gloss achievable by a given coating layer as rms surface roughness approaches zero, i.e. $\sigma \to 0$. The absolute value of the argument in the exponential term, g_R, is the Rayleigh parameter; as defined by Equation (9), that signifies the degree of light scattering at the surface.

Oittinen argued that roughness of coated paper arises from two sources: the coating itself and the base paper [86]. Generally, roughness of paper is two orders of magnitude larger than the wavelength of light while the roughness due to coating pigments is of the order of wavelength of light. Accordingly, a two-scale model was proposed where the total light reflection was assumed to be the product of the contribution due to the optical roughness (originating from the coating layer) and that of microscopic roughness (originating from the base paper nonuniformity). In addition to surface roughness, Oittinen showed that the local gradient of surface heights also affects the gloss of paper. In a subsequent study, Lipschitz and co-workers used an optical surface profilometer and reported that the distribution of local slopes,

or facet angle distribution, correlates well with changes in the gloss values of coated papers [87]. Furthermore, it was found that facet angle could explain 78% of the measured gloss variation [88], and that there is a good correlation between mean facet angle and visual ranking [89]. Chinga explored the relationship among various surface descriptors and gloss using multivariate analysis [90]. He reported that gloss correlated well with the median facet angle as well as surface pore volume while the conventional Parker Print-Surf (PPS) roughness was only weakly related to the gloss (Figure 14). Chinga and co-workers later examined this observation and proposed that PPS roughness is mostly affected by surface features on the order of 80–160 μm, while gloss is dominated by micro-structures below 12 μm [91]. Hence, by representing the surface of paper as a collection of micro-facets, several researchers developed mathematical models to estimate the intensity of scattered field. For a polarized collimated incident beam of light I_o, and assuming that light reflection from each fact follows the laws of geometrical optics, one can show that the intensity of scattered light, $I_s(\theta_s, \varphi_s$, over the solid angle is $d\omega_s$ [20]:

$$I_s(\theta_s, \varphi_s)\, d\omega_s = I_o\, R_F(\theta, n)\; f_f\left(\theta_f, \varphi_f\right) d\omega_f \tag{58}$$

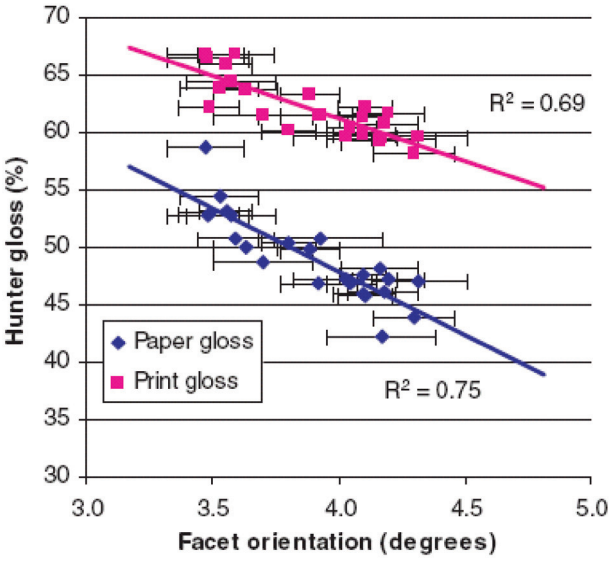

Figure 14. Relationship between paper and print gloss with the facet angle of unprinted SC papers [91].

where $f_f(\theta_f, \varphi_f)$ is the distribution of facet angles and $R_F(\theta, n)$ is the Fresnel coefficient based on the local angle of incident θ. Following Oittinen's model, Elton and Preston suggested that the overall light reflection is the result of two contributions: macroroughness and microroughness of paper. Hence, the s-polarized light intensity, I_s, was suggested to be :

$$I_s(\theta_s, \varphi_s)\, d\omega_s = I_o\ \exp(-g_R)\, R_s(\theta, n)\, f_f\left(\theta_f, \varphi_f\right) d\omega_f + \ dI_v \qquad (59)$$

The term dI_v represents the contribution of subsurface multiple scattering. A similar equation may be obtained for the *p*-polarized illumination. Using the above equation, the authors reported a good correlation between the measured and predicted gloss values. In their case, gloss was measured using an imaging reflectometer (Figure 5). Elton and Preston also examined the effective refractive index of coated papers and found that for a given pigment type the refractive index decreases linearly with the mean pore diameter [92].

Hansson used an angle resolved light scattering measurement method to analyze a wide range of commercial papers [14]. This device used a 2 mm^2 He-Ne laser beam as illuminant and a rotating sample holder to detect the angular distribution of scattered light. Using geometrical optics to estimate the surface reflection and Lambert's law for the bulk (subsurface) reflection of paper, he proposed the following expression for the intensity of scattered light:

$$I_s(\theta_s, \varphi_s) = \frac{I_o}{\pi}\left[R_d \cos\theta_i + \frac{R_s}{8\,\sigma_s} \exp\left(-\frac{(\theta_s - \theta_i)^2 + {\varphi_s}^2}{8\,{\sigma_s}^2}\right)\right] \qquad (60)$$

where R_d and R_s are the diffuse and specular reflectance coefficients, θ_i is the illumination angle, and σ_s is the standard deviation of surface slopes. Figure 15 shows the experimental and predicted microgloss images of a light-weight coated paper sample based on Equation (60).

In studying laboratory coated papers with gloss values ranging from about 20% to above 80%, Caner *et al.* reported that Rayleigh parameter, g_R, varied from 5 to more than 800 [94]. They demonstrated that under such conditions, as expected, the smooth surface approximation described by Equation (57) was no longer applicable. Instead, gloss was a function of both rms roughness and correlation length, L_c, of the surface topography. This is consistent with the earlier findings of Alexander-Katz and Barrera who reported that the surface height correlation cannot be neglected in the prediction of gloss [93]. To better illustrate the significance of correlation length on the topography, Figure 16 illustrates two Gaussian random surfaces with the same rms roughness but different correlation lengths and their corresponding diffuse

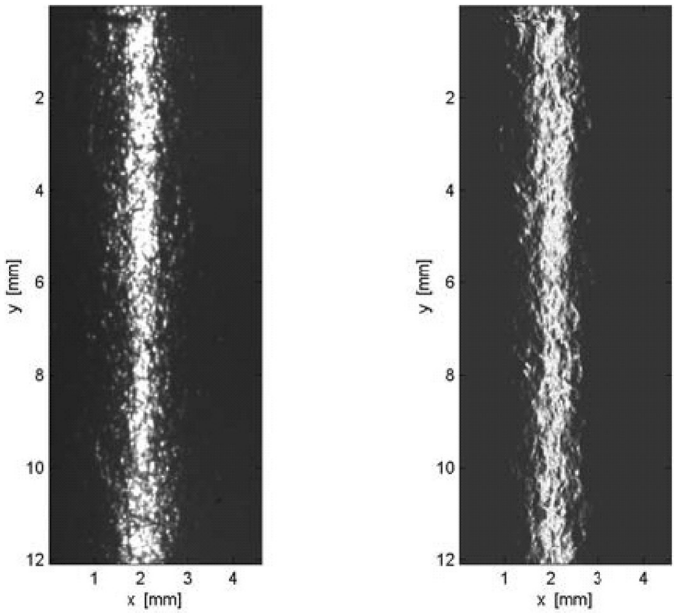

Figure 15. Experimental (left) and simulated (right) microgloss images of a light weight coated paper [14].

scattered field intensities. Caner *et al.* found that gloss of coated papers is a function of surface texture parameter, L_c/σ^2, according to the following semi-theoretical expression:

$$G_\theta = b\,(L_c/\sigma^2)^n \tag{61}$$

Values of b and n for various standard gloss angles, θ, are given in Table 4. Despite wide variations in the surface roughness and coating formulations (including fourteen clay and GCC pigments), the above equation was able to

Table 4. Values of b and n for equation (61).

Gloss Angle, θ	*B*	*n*
20°	0.5	0.41
60°	4.1	0.52
75°	19.3	0.31

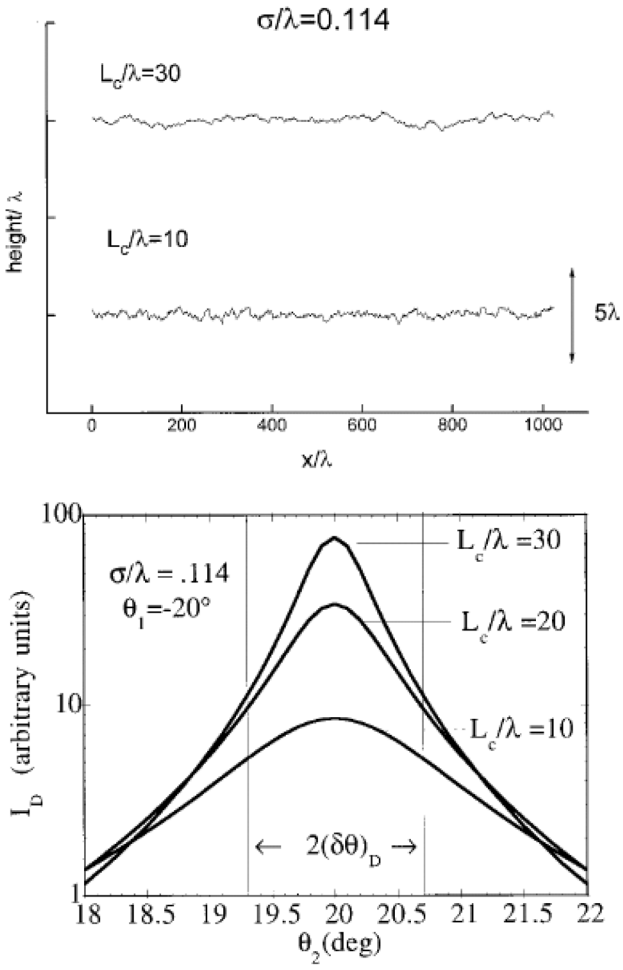

Figure 16. Top: simulated random surface profiles for a Gaussian distribution of heights and an exponential height correlation function for $\sigma/\lambda = 0.4$. λ is the wavelength of light, bottom: effect of correlation length on the diffuse scattering field [93].

predict the standard gloss with a regression coefficient ranging from 0.61 to 0.78 (Figure 17).

It should be pointed out that the values of rms roughness and correlation length in Equation (61) were measured using an interferometric profilometer

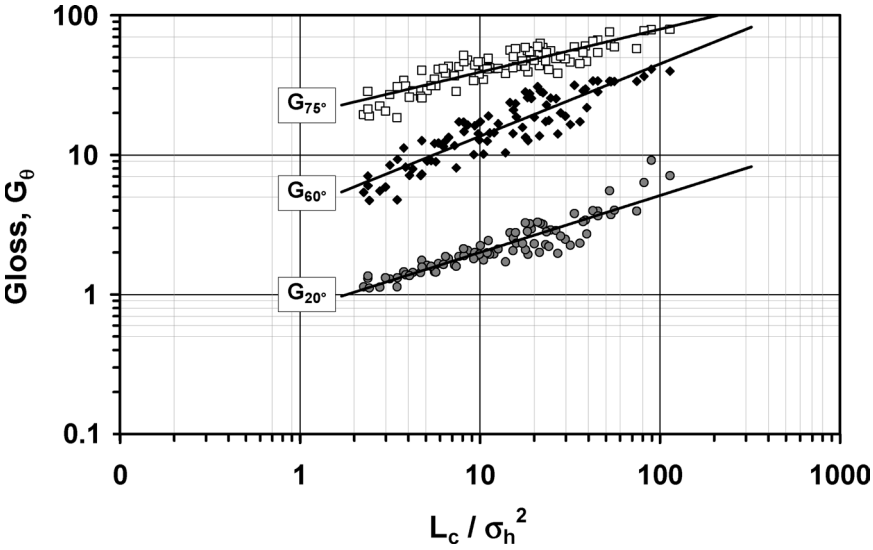

Figure 17. Relationship between standard gloss and surface texture parameter, L_c/σ^2, at three gloss angles [94].

(WYKO NT2000) over an area of 460 × 680 μm^2 with a horizontal resolution of 0.82 μm. However, the surface statistics of paper are dependent on the measurement resolution and sampling area. To illustrate this effect, Figure 18 shows that by increasing the measurement size up to 6 mm, the rms roughness for a coated paper sample increased and reached a near-plateau after about 2 mm. In contrast, the correlation length continued to increase with the sample size and at 6 mm reached nearly 500 μm; three orders of magnitude greater than the wavelength of visible light. A similar trend has been reported elsewhere for several office papers over a measurement length of 1.5 mm [95, 96]. These observations have significant implications in terms of applicability of various wave scattering theories and they also illustrate challenges involved in the measurement of surface topography of paper. In an attempt to identify the suitable resolution that is optically responsible for gloss, Vernhes *et al.* compared the experimental scattering indicatrix with the predicted values using a virtual goniometer [97]. Their study showed that the best fit between experimental and measured values was obtained if the surface was measured at a high magnification.

With recent advancements in computational speed, structure-based modeling of paper optical properties is becoming increasingly affordable. For example, Green *et al.* studied the angle-resolved light reflectance from paper

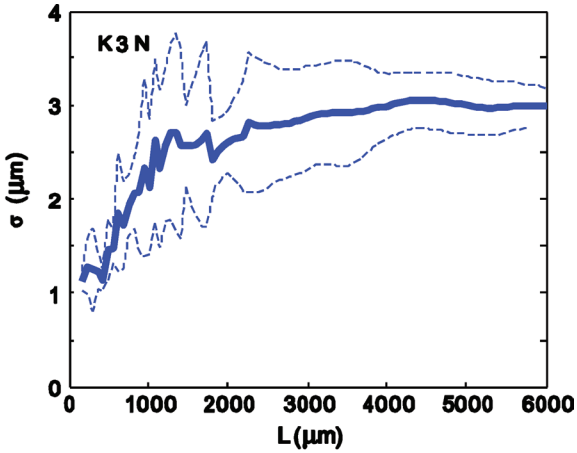

(a)

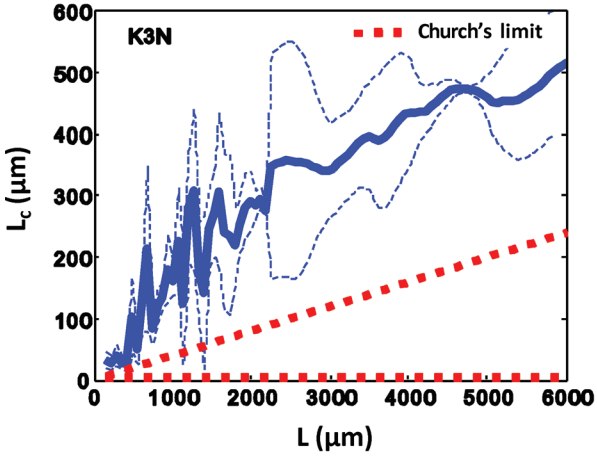

(b)

Figure 18. Dependence of rms roughness (a) and correlation length (b) on the sample size, L, measured by an interferometric profilometer. Sample is a kaolin coated papers with 10 pph SB latex and lateral resolution is 0.82 µm [99].

based on geometrical optics (ray tracing) techniques and Monte Carlo simulation. They modeled paper as a three-dimensional network of randomly distributed cylindrical fibres with varying dimensions (i.e. length, diameter, fibre wall thickness) and orientations [98]. Although the geometry used in this

study was a crude representation of paper structure, their study was a significant step towards the prediction of paper's optical properties based on paper structure and furnish.

A fact that is commonly overlooked in gloss measurements is the dependency of the measured gloss value on the angle of acceptance of detector, $\delta\theta$. Oittinen found that the measured gloss values for a polished black glass increased linearly and reached a plateau by increasing $\delta\theta$. However, it is to be expected that this dependency would be significantly different for rough surfaces such as commercial papers. To study this effect, Arney and co-workers proposed that gloss may be estimated using a circular BRDF function [100]:

$$G(\theta) = \frac{1}{K}\int_{-\delta\theta}^{+\delta\theta} R_F \frac{w_o F}{w_0^2 F^2 + \alpha^2}.d\alpha \tag{62}$$

Here, w is the half width of BRDF, and K is the area under the BRDF for the reference material. The angle of acceptance of the gloss meter was estimated by reverse engineering. By ignoring shadowing effects, authors were able to predict the experimental gloss data and show that the angle of acceptance of the gloss meter had a strong effect on the predicted gloss values.

Modelling gloss of rough surfaces using KA

Using scalar Kirchhoff theory and assuming surface height is a stationary Gaussian random variable with a modified exponential correlation function, Lettieri *et al.* studied the reflection of light from the surface of coated papers [40]. The authors found a good correlation between the angle-resolved light scattering data and the model predictions. In a later study, Alexander-Katz and Barrera developed analytical models for light reflection from stationary Gaussian surfaces with either Gaussian or exponential autocorrelation functions. With some simplifying assumptions, for the asymptotic case where surface is rough (i.e. $g_R \gg 1$), and where surface slope ($\approx \sigma/L_c$) is large enough to create a nearly isotropic diffuse field, they obtained the following expression for the specular gloss [93]:

$$G(\theta) = 100\,\frac{R_F}{R_{F,o}}\frac{y_D^2}{2}\exp(-g_R)\;\cos\theta\left(\frac{\Omega_{\mathrm{D}}}{\pi\,(\delta\theta)^2}\right)\int_0^{\infty}(\exp(g_R\exp(-x^m))-1)\,x.\,dx \tag{63}$$

Here, $\delta\theta$ is the detector collecting half-angle, R_F and $R_{F,o}$ are the Fresnel reflectance values of the sample and that of the standard, Ω_{D} is the solid angle of acceptance of the detector, and y_D can be expressed as:

$$y_D = \frac{2\,\pi}{\lambda}\, L_c\,(\delta\theta) \tag{64}$$

In Equation (63), m is a constant that depends on the form of the surface height autocorrelation function. The value of m is equal to 1 for the exponential correlation function and 2 for Gaussian correlation function.

For large values of the Rayleigh parameter, the integral term in this equation can be further reduced to give the following simple expression for gloss:

$$G(\theta) \cong 100\,\frac{R_F}{R_{F,o}}\,\frac{y_D^2}{2\,m\,g_s^{2/m}}\cos\theta\,\left(\frac{\Omega_{\mathrm{D}}}{\pi\,(\delta\theta)^2}\right) \tag{65}$$

For an exponential autocorrelation function (m = 1), Equation (65) predicts that the specular gloss is proportional to L_c/σ^2. This contradicts experimental observations that gloss is a nonlinear (power-law) function of L_c/σ^2. To resolve this issue, we recently proposed an analytical expression for the gloss of paper based on first-order Kirchhoff approximation [41]. A detailed derivation of this model is provided below.

As discussed earlier, in the Kirchhoff approximation, the scattered field could be fully characterized based on the incident illumination, surface topography, and the Fresnel coefficients. In this case, assuming that the scattered field is concentrated around the specular direction, the components of scattered field are given by [101]:

$$E_s = \frac{j\,k_o\exp(j\,k_o R_o)}{4\,\pi\,R_o}\,E_o\,I_1\,F \tag{66}$$

where E_o is the amplitude of incident field, R_o is the distance from the surface to the detector, k_o is the incident wave number, I_1 is a function that depends on the position and elevation, and F is a function of Fresnel coefficients and measurement geometry.

Bourlier and Berginc estimated the elevation difference between two adjacent points using $z_i - z_i \approx \mathbf{s}_j\,.\,(\mathbf{r}_i - \mathbf{r}_j)$, where $\mathbf{s}_j = s_{jx}\vec{x} + s_{jy}\vec{y}$ is the local surface slope and (see Figure 19):

$$\begin{aligned} s_x &= (\sin\theta_s\cos\varphi_s + \sin\theta_i)/\,(\cos\theta_s + \cos\theta_i) \\ s_y &= \sin\theta_s\sin\varphi_s\,/\,(\cos\theta_s + \cos\theta_i) \end{aligned} \tag{67}$$

Based on this approximation and by ignoring the shadowing effects, the scattered intensity becomes:

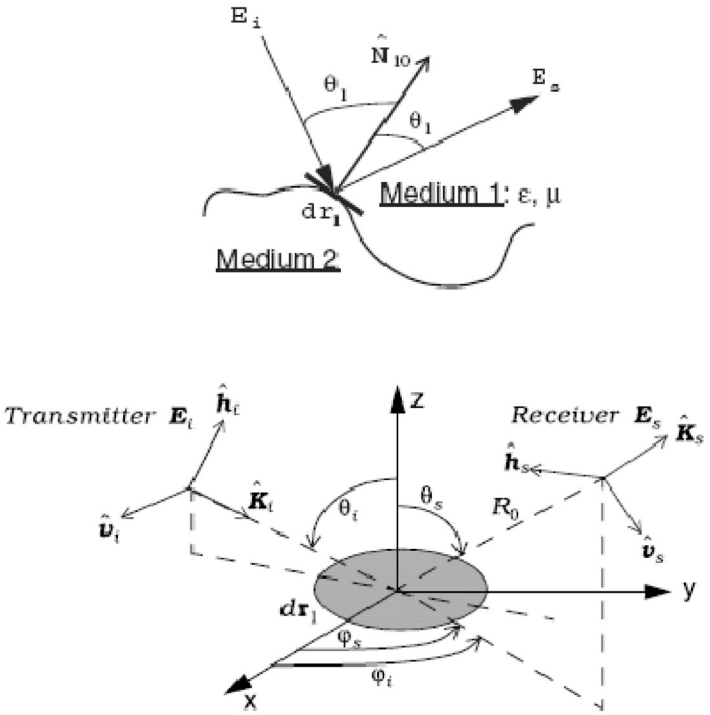

Figure 19. Top, first order Kirchhoff (or tangent plane) approximation, and bottom incident and scattered fields geometry [101].

$$I_s = \frac{A\,|E_o|^2}{4{R_o}^2}\,\frac{|F|^2}{(\cos\theta_s + \cos\theta_i)^2}\;\; f_s \tag{68}$$

where A is the illumination area and f_s is the probability distribution function of slopes. For a given glossmeter, the incident intensity and geometrical parameters remain constant. Hence, recalling that gloss is the ratio of the specular reflection of the sample to that of a reference material, the specular gloss measured by a receiver with angles of acceptance of ($\pm\delta\theta$, $\pm\delta\varphi$), is given by:

$$G(\theta) = G_o \int_{-\delta\theta}^{+\delta\theta} \int_{-\delta\varphi}^{+\delta\varphi} f_s \, d\varphi . d\theta \tag{69}$$

Theoretically, G_o is the limiting value of gloss for a perfectly smooth surface and hence can be determined from the Fresnel equation. To evaluate the above equation, it is assumed that surface slopes in x and y directions are independent and identically distributed exponential random variables with the standard deviation of σ_s, i.e.:

$$f_s(s_x, s_y) = \frac{1}{2\sigma_s^2} \exp\left(-\frac{\sqrt{2}|s_x|}{\sigma_s} - \frac{\sqrt{2}|s_y|}{\sigma_s}\right) \tag{70}$$

$$G(\theta) = G_o \int_{-\delta\theta}^{+\delta\theta} \int_{-\delta\varphi}^{+\delta\varphi} \frac{1}{2\sigma_s} \exp\left(-\frac{\sqrt{2}|s_x|}{\sigma_s} - \frac{\sqrt{2}|s_y|}{\sigma_s}\right) d\varphi . d\theta \tag{71}$$

The rms of the surface slopes may be either calculated directly from topographical data, or estimated recognizing that $\sigma_s = 2\,\sigma/L_c$ [102].

Integration of Equation (71) provides an estimation of the gloss. However, further simplification can be considered to derive closed-form analytical expressions. In the case of specular gloss, the angle of acceptance of the receiver is relatively small. Hence, based on Taylor expansion and neglecting higher order terms, one can obtain:

$$\begin{aligned} s_x &\approx \frac{1}{2}\,\delta\theta \\ s_y &\approx \frac{1}{2}\tan\theta_i\,\delta\varphi \end{aligned} \tag{72}$$

Finally, from (71) and (72), the following approximation for the specular gloss is obtained:

$$G(\theta) \approx G_o \left(1 - \exp\left(-\frac{\delta\theta}{\sqrt{2}\,\sigma_s}\right)\right)\left(1 - \exp\left(-\frac{\delta\varphi \tan\theta_i}{\sqrt{2}\,\sigma_s}\right)\right) \tag{73}$$

Although Equation (73) is derived for rectangular apertures, numerical studies have shown that it provides a good estimation of gloss for circular detector geometries by assuming $\delta\theta = \delta\varphi$.

As was pointed out earlier, theoretically, G_o is the limiting value of gloss for a perfectly smooth surface (i.e. $\sigma_s = 0$). However, here, this value was treated as a constant value and was determined by fitting the experimental data. Figure 20 shows the comparison between experimental data and predicted gloss values for 47 coated and uncoated samples with standard 75° Tappi

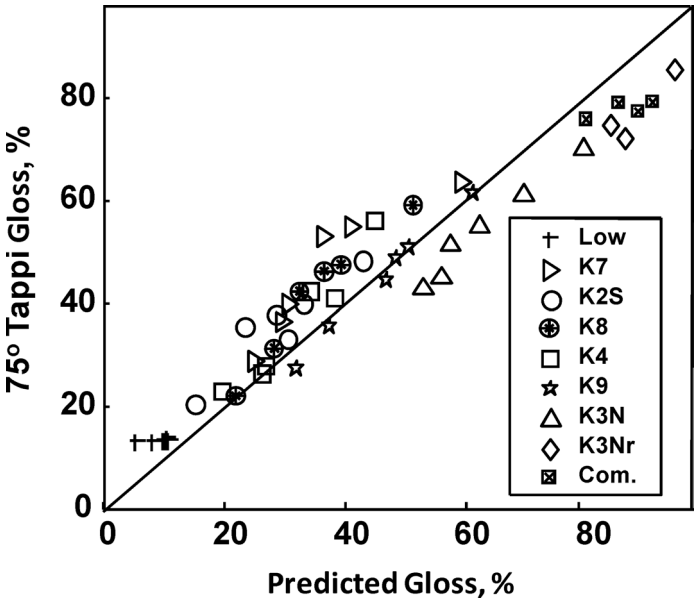

Figure 20. Comparison between experimental and predicted 75° Tappi gloss values for laboratory and commercial coated papers based on Equation (73) [41].

gloss values of about 6 to 87. Equation (73) provides a good fit to experimental data ($r^2 = 0.94$).

The above theoretical and experimental studies emphasize the importance of material characteristics as well as measurement conditions on the gloss value. Moreover, it is clear that the intensity of reflected light in the specular direction is a nonlinear function of surface parameters; i.e. roughness, correlation length, and facet angle. At first, this latter conclusion may appear to disagree with the recent results of Järnström *et al.* who found the gloss of coated films varied linearly with the rms roughness [103]. However, the roughness values in Järnström's study were in the range of nanometers and hence their samples may be considered optically smooth. Although the study of gloss of optically smooth coated films with roughness values of the order of wavelength of light has been used traditionally to gain useful fundamental information [85], in practice, the surface roughness of coated paper is modulated by base sheet nonuniformities that are several orders of magnitude larger than the wavelength of visible light.

Bulk scattering effects on gloss

Conventionally, it is believed that gloss is created at the uppermost layer of paper, i.e. within a thickness smaller than half the wavelength of light [104]. Previous studies have shown that the gloss of coated papers is predominantly a surface-dependent parameter. Therefore, in theoretical analysis of gloss, the effect of bulk properties of coating and paper are commonly ignored. Although this may be a good first approximation, evidence suggests that the choice of base paper and pigment characteristics can also affect gloss and local gloss variability through bulk scattering effects. Experimentally, the influence of bulk and surface scattering on gloss may be isolated using polarized light reflectrometry [105, 106]. Based on this method and using the set-up described earlier (Figure 4), we recently measured the surface and bulk microgloss for a wide range of laboratory coated papers. These samples were coated on one side with six different formulations (including three kaolin pigments and three GCC pigments) and were calendered to various degrees to achieve a range of Tappi gloss from 10% to about 65%. Figure 21 shows the measured contributions of bulk and surface scattering to the total measured microgloss. Interestingly, regardless of coating formulations and calendering treatment, all samples followed the same trend lines. Surface microgloss increased linearly as total microgloss increased while the bulk microgloss remained nearly constant at about 100 grey level unit (corresponding to a contribution of about 10% to the total Tappi gloss). At microgloss values below about 250 grey level unit (GL), corresponding to a Tappi gloss of about 30%, the measured total gloss values were dominated by the bulk scattering effects. Further work is currently being undertaken to better understand these phenomena.

Print gloss

Print gloss has a direct impact on the perception of print quality. Print gloss is measured similar to paper gloss. This is a complex parameter that is affected by paper properties, including pore structure, roughness, and surface chemistry, and printing conditions, such as ink type and printing method. Moreover, ink-paper interactions play a significant role in determining the final gloss of printed papers. In the case of coated papers, it is generally believed that the ink film covers small irregularities and hence enhances the gloss. However, it is also known that ink film can add to irregularities through filament patterns produced during ink splitting [108] or due to ink pigments that protrude from the smooth ink layer [109].

MacGregor and Johansson analyzed a wide range of unprinted and printed coated papers and reported that there was virtually no correlation

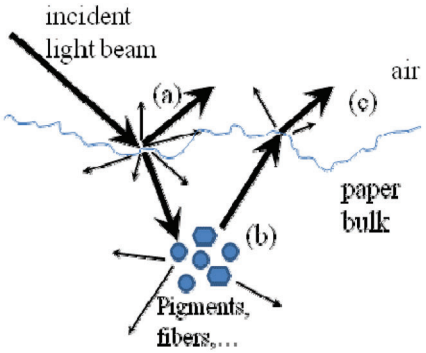

(a)

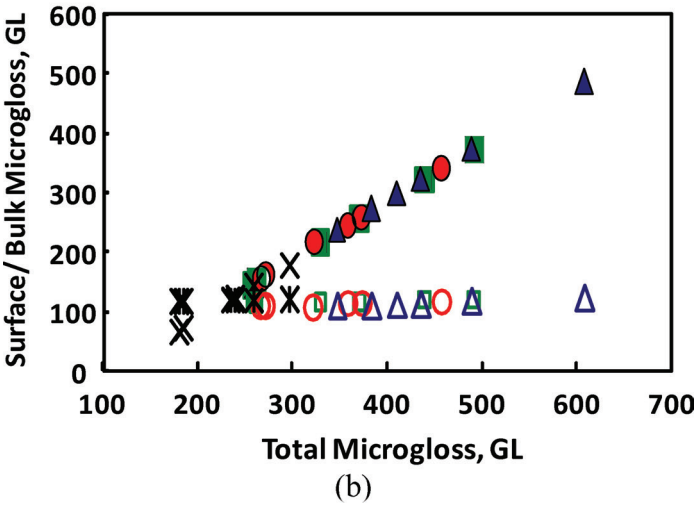

(b)

Figure 21. (a) schematic illustration of bulk and surface scatteing effects on the total scattered field, and (b) surface and bulk microgloss of coated paper samples in grey level units (GL) [107].

between print gloss and gloss of the base paper [110]. In contrast, Ström *et al.* found a strong correlation between the print gloss and the roughness of unprinted paper measured in PPS [111]. In a different study, Donigian *et al.* observed that print gloss and paper gloss exhibited opposing trends with

decreasing the size of calcite precipitated calcium carbonate (PCC) [112]. They also reported that fewer larger pores resulted in higher print gloss, and that coating absorbancy could overwhelmingly affect the print gloss by masking any gain in the paper gloss. Similarly, for offset printed coated papers, it has been reported that print gloss is affected by the surface pore structure [113] as well as ink levelling and resin deletion [114]. These sometimes contradictory observations emphasize the importance of printing conditions and ink-paper interactions to the gloss of printed papers.

Similar to paper gloss, print gloss is a function of the surface roughness. Using frequency domain analysis, Matsuda *et al.* suggested that the surface of printed paper could be considered as a cluster of sine waves with various frequencies and amplitudes [115]. They reported that surface profiles with spatial frequencies more than 30 or 40 mm^{-1} can significantly affect paper gloss. They also found that gloss of printed papers was affected by a larger range of spatial frequencies than that of unprinted papers, and hence suggested that by increasing the high frequency component and reducing the low frequency contribution to roughness it may be possible to increase the delta-gloss of matte coated grades. Ström and co-workers studied the coated offset prints and concluded that print gloss had a strong correlation ($r^2 = 0.82 - 0.90$) with both PPS and the "sub-macro" roughness, i.e. roughness measured over $100 \times 100\ \mu m^2$ using AFM [111]. Furthermore, using Fourier analysis they reported that base paper roughness at the scale of 50 – 250 μm was predominantly responsible for the observed print gloss. In a later study, Ström and Karathanasis found that the relationship between print gloss and micro-roughness of unprinted paper virtually disappeared after 3 – 4 g/m^2 of ink was applied on the surface of coated paper, but a strong linear relationship was found between print gloss and micro-roughness of prints [116]. They also observed that increasing the amount of ink applied on a fast setting substrate increased the roughness and created a non-linear relationship between print gloss and the applied amount of ink due to the formation of ink filament patterns.

Using the microgloss setup described earlier (see Figure 4), we studied the effect of the surface texture of printed papers on the print gloss. Figure 22 shows the micro-gloss of laboratory-made and commercial unprinted coated paper (lower line) and commercial offset printed coated papers (upper line). Similarly to paper gloss, print gloss was found to exhibit a power-law relationship with the surface texture parameter, L_c/σ^2. It is also important to note that the gloss of printed samples is consistently higher than that of unprinted papers at the same value of L_c/σ^2.

Arney *et al.* used their imaging micro-goniophotometer (Figure 3.a) to study the gloss of paper and prints, and found that the reflectance of black electro-photographic prints closely followed the Fresnel equation with an

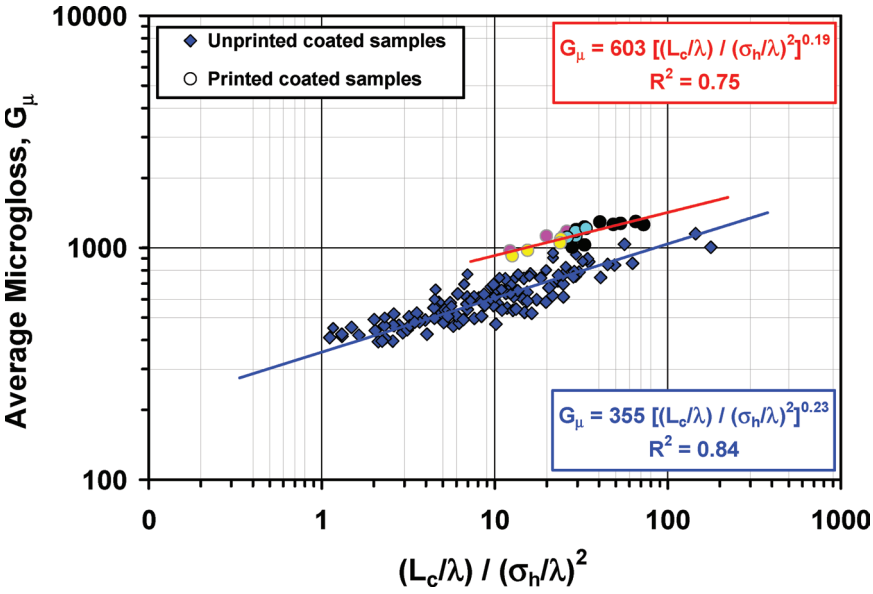

Figure 22. Microgloss of laboratory and commercial coated papers (lower line) and commercial offset prints (upper line) as a function of L_c/σ^2 [117].

extinction coefficient of 0 [17]. Using the same setup, Arney and co-workers studied the effect of color on gloss. Conventionally, gloss of prints is considered to be the same color as the illuminant. However, by measuring the relative area under the bidirectional reflectance distribution function, Arney *et al.* found that the relative reflectance of color inks was not only a function of the illumination color but also depended on the ink type (Table 5) [16]. In

Table 5. Relative area under BRDF for various inks under different illumination color [16].

Color of Incident Light	*Type of Ink*			
	Cyan	*Magenta*	*Yellow*	*CMY*
Red	1.2	1.7	1.4	1.0
Green	1.4	1.2	1.3	1.0
Blue	1.5	1.2	1.2	1.0

addition, the amount of specular reflection was found to be a strong function of the optical density of ink, such that more transparent inks were found to be more reflective than absorbing inks. This seems to be counterintuitive since a highly absorbing material is expected to have a higher refractive index, and according to Fresnel's law, will cause a higher reflectance. The authors explained their results by suggesting that specular reflection occurs in more than one interface and that reflection from the substrate had a significant contribution to the overall gloss. They proposed a three-layer model where the ink layer is in optical contact with air (instead of direct contact with paper), and hence the overall reflectance is the sum of reflectances from the air-ink (R_i), ink-air, and air-paper (R_p) interfaces. Defining the transmittance of the ink layer as T, and assigning $T = 0$ for cyan-magenta-yellow (CMY) ink, the relative reflectance with respect to the black ink, r, was estimated to be [16]:

$$r = 1 + \left[(1 - R_i)^2 T^2 + (1 - R_i)^4 T^2 \, R_p / R_i\right] \times F_A \tag{74}$$

where F_A is an attenuation factor that is treated as a fitting parameter. According to Equation (74), the relative reflectance of printed samples is a linear function of the square of the ink's transmittance. This relationship was confirmed by the experimental data presented by the authors.

Gloss nonuniformity

Both the average gloss and the gloss nonuniformity affect the visual perception of paper and prints. Using an x-y scanner with 400 μm spot size, Fujiwara *et al.* analyzed a wide range of commercial coated papers and showed that the gloss uniformity had the strongest impact on the appearance of unprinted coated samples [118]. In their study of commercially printed coated papers, MacGregor and Johansson found that the visual ranking of printed papers correlated well with gloss variations in the range of 200 μm to 1600 μm [110]. However, evidence suggests that the scale of gloss variation that is primarily responsible for the visual ranking may depend on the type of samples and the visual assessment method. For example, Béland *et al.* reported that gloss variations in the 3.3 mm to 6.6 mm range correlated best with the visual ranking of 32 commercial offset prints of matte-coated papers [89].

It has been shown that the gloss nonuniformity of printed paper corresponds to variations in the local roughness of print [119]. Using atomic force microscopy, Béland and Bennett found that low gloss areas of a printed sample were 3 to 4 times rougher than the high gloss areas. They also

identified low gloss regions that were either smooth but tilted or flat but rough. MacGregor suggested that up to potentially 90% of the gloss variation was accounted for by topography, and proposed that gloss evaluation methods need to improve in order to capture the texture effects on the visual perception of gloss variability [120].

In a recent study, we investigated the microgloss variation of coated samples as a function of pigment type, as well as calendering load and temperature [117]. It was found that for a given coating formulation and base sheet, microgloss variation was governed by the surface texture parameter, L_c/σ^2. However, as seen in Figure 23, this relationship was also dependent on the pigment type. Figure 22 and Figure 23 suggest that by appropriate selection of coating pigment, it is possible to achieve the same level of gloss with lower micro-gloss variability.

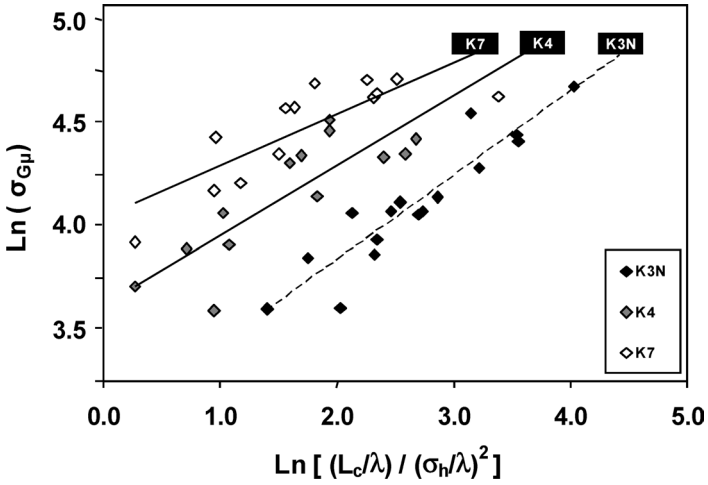

Figure 23. Log-log relationship between the standard deviation of microgloss, $\sigma_{G\mu}$, and surface texture parameter, L_c/σ^2, for three kaolin pigments. Pigment size and morphology are K7 : 0.22μm, undelaminated; K4: 1.18 μm, delaminated, K3N: 2.16, delaminated [121].

FILLERS AND PIGMENTS

Papermaking furnish, together with finishing and converting processes, determines the optical performance of paper products. A recent review of papermaking practices that affect the appearance of paper can be found in

[122]. An effective method to enhance the appearance of paper is through the use of mineral pigments for coating and internal filler applications. Fillers enhance the optical properties of paper by improving the light scattering capacity through increasing the specific surface area. A review of pigment characteristics and applications in papermaking can be found elsewhere [123]. Due to higher cost and reduced availability of raw materials, there has been a tendency to substitute fibres with fillers. Fillers are traditionally introduced to the wet end of papermaking and are retained in the sheet during the dewatering process. Increasing the filler content adversely affects the mechanical properties of paper. An alternative method of incorporating fillers in the sheet is through lumen loading [124–126]. Compared to traditional methods for filler addition, lumen loading allows for a higher mechanical strength at the same amount of filler content; however, this method demonstrates a lesser degree of improvement in optical properties (Figure 24).

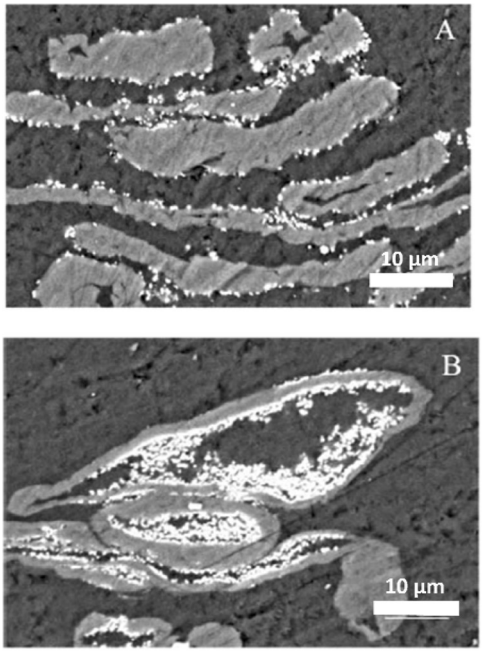

Figure 24. SEM cross section showing the calcium carbonate distribution in, A) conventionally filled handsheet with 13% filler, and B) lumen loaded sheet with 22% filler [125].

Pigment coating, on the other hand, improves the surface finish of paper. In recent years, higher demand for improved brightness and opacity has resulted in the increasing introduction of calcium carbonate as a coating pigment. At the same time, as with fillers, there is a trend towards greater pigment to fibre ratios [127]. The main pigment characteristics that affect the appearance of paper are pigment particle size and particle size distribution (PSD), as well as pigment shape, brightness, color, refractive index, scattering, and morphology. Significant advances have been made in designing novel pigments with improved brightness, opacity and gloss by optimizing pigment size, morphology and structure. Proper choice of pigment and calendering conditions is of the utmost importance for the trouble-free production of paper with desirable attributes.

Table 6 provides a summary of recent studies related to the effect of coating and calendering conditions on the optical properties of coated papers. This table shows that both calcium carbonate and kaolin clay are widely used in today's papermaking. Kaolin clay remains a popular mineral for filler and coating applications. Clay has a good color (white or near white) and a fine particle size. It is inert, non-abrasive, and readily dispersible in water. Optical properties of clay can be significantly enhanced by engineering clay products through chemical and thermal treatment methods [128, 129]. A recent shift towards alkaline papermaking has resulted in an increased utilization of calcium carbonate in the wet-end and as coating pigment. Calcium carbonate used in papermaking is either produced by grinding natural limestone, chalk, or marble (GCC) or through a precipitation process (PCC). GCC has rhombohedral morphology; however, the morphology of PCC can be adjusted. Scalenohedral PCC is the most widely used morphology as filler [130]. The higher brightness, whiteness, and light scattering coefficient of calcium carbonate when compared to clay may produce a base paper with better optical properties. However, this is not always true, since, for example, the use of calcium carbonate as filler may lead to a more porous and rougher base sheet that will offset any gain in the optical properties of finished product [131]. Figure 26 illustrates the range of brightness values for commercial papermaking fillers.

Scattering coefficient of fillers and coatings

The ability to scatter visible light is an important attribute of fillers used in papermaking. A high scattering coefficient is desirable for the optical properties of paper such as opacity, brightness, and whiteness. The scattering coefficient of pigments/fillers is not only a function of their size, size distribution, morphology, and refractive index, but is also affected by the packing

Table 6. Summary of recent studies related to the effect of coating formulation and calendering conditions on the optical properties of coated papers.

Ref.	*Pigment*	*Variable*	*Summary of Results*
[132]	Clay, PCC	Pigment type	Adding prismatic PCC to platy clay and decreasing latex content lowered gloss.
[133]	Aragonite PCC	Pigment Particle Size	Brightness, paper gloss, and print gloss decreased and opacity increased with particle size.
[134]	GCC or PCC + Ultra Fine Clay	Calendering Moisture	Gloss increased with sheet moisture.
[112]	Calcite PCC, Clay	Particle size distn., Binder content	Reducing particle size, increased paper gloss but decreased print gloss. Latex content did not have a consistent trend on gloss. Adding 50% clay to formulation improved gloss.
[135]	Unknown	Coating method	Gloss changed in the following order: Blade Coating > Film coating > Curtain Coating.
[136]	TiO_2 Rutile & Anatase, ZnS	Pigment type and loading	At the same target brightness, opacity increases as: Rutile > ZnS > Anatase.
[78]	TiO_2	Coating Pore Structure	Light scattering increased by increasing the pore diameter and peaked at about 400–450nm.
[137]	GCC + Clay	Base paper, Filler content, Pre-calendering, Coating method	Film coating had lower gloss than blade coating. Higher filler content and better formation had lower gloss variability. PGW had higher opacity than TMP, and precalendering reduced opacity.
[138]	GCC, Clay	Pigment type, Calendering conditions	Pigment size and shape have strong influence on gloss. The broadness parameter had no significant influence on the gloss.

[121]	GCC, Clay	Pigment Characteristics, Calendering Conditions	Pigment size distribution affected both microgloss and microgloss nonuniformity. Higher gloss results in higher microgloss nonuniformity, and this relationship depends on the pigment type. Gloss nonuniformity of GCC is more sensitive than kaolin. Higher calendering temperature increased gloss and gloss nonuniformity.
[139]	Clay+ GCC + Hollow/ filled plastic pigment	Pigment type	Increased hollow sphere pigment increased reflectance and gloss. Hollow sphere increased brightness and scattering coefficient more effectively than filled spherical pigments.
[140]	GCC, PCC, Clay	Pigment type	Aragonite PCC outperformed GCC. At the same target gloss, PCC had higher opacity & brightness. PCC coated sheet had higher gloss at lower calendering levels
[141]	GCC	Latex dispersion	Better dispersion of latex in the coating layer improved gloss.
[142]	Scalenohedral PCC, porous PCC, GCC	Pigment morphology	High light scattering, and high opacity and brightness were achieved using porous PCC compared to GCC. Increasing coat weight from 8 to 16 gsm increased brightness of PCC but not GCC.
[143]	PCC + Fine Clay	Pre-calendering temperature	Increasing pre-calendering temperature increased gloss due to better coverage.
[144]	GCC	Latex type, Calendering speed	Latex with higher gel content gave higher gloss. Higher web temperature increased the gloss. Higher calendering speeds lower the gloss.
[145]	GCC, Clay	Coating structure, Latex content Pigment type	Gloss increased linearly with the reduction in pore diameter. Correlation between gloss and the reduction in pore volume was poorer. Higher latex content decreased gloss of precalendered sheet, but had no effect on the gloss of calendered paper. Clay has higher gloss than GCC (with similar PSD) before and after calendering.

Table 6. Continued

Ref.	*Pigment*	*Variable*	*Summary of Results*
[146]	GCC+Clay blends	Pigment blend	Gloss increased linearly by increasing clay content. Light scattering coefficient increased by clay addition and peaked about 80–90% clay for calendered and uncalendered sheets.
[147]	Aragonite PCC Clay	Pigment shape factor	Gloss is mostly affected by pigment size than the shape factor. Light scattering coefficient was the same for all clay coatings, but much higher for aragonite PCC.
[131]	GCC + Clay or Engineered Clay	Filler content	Increasing filler content from 5% to 15% had the same effect on brightness as replacing clay with engineered clay, but with a higher paper and print gloss. Compared to kaolin coating, GCC had a more open structure hence higher light scattering but rougher surface and hence lower gloss.
[75]	GCC + Clay	Pigment blend Pigment size distn.	GCC with narrow particle size distribution had the highest contribution to the brightness, while GCC with broad particle size distribution had highest contribution to whiteness.
[148]	Delaminated Clay Calcined Clay Talc	Pigment Blend	Gloss was reduced with increase in talc or calcined clay content. At equal calendering and equal gloss conditions, brightness increased with delaminated clay and decreased with talc. At equal gloss levels, opacity improvement was quite significant for delaminated clay over talc
[149]	Clay+GCC + Talc	Pigment blend	Replacing clay # 1 with talk in a matte coated art paper, increased print gloss but decreased paper gloss.
[150]	Narrow PSD GCC, PCC, Fine GCC	Pigment type and binder content	Higher latex decreased gloss, whiteness and brightness of a coated board. However, print gloss increased with latex content. Gloss, whiteness and brightness decreased as: PCC>Narrow PSD GCC >Fine GCC

[151]	GCC, PCC, Kaolin	Pigment blend, calendering load	Brightness increased by increasing the coating pore size while print gloss and delta gloss require a balance between pore size and pore volume.
[152]	GCC, Kaolin	Latex type, Calendering load and temperature	Higher calendering temperature had a higher paper and print gloss. Extended nip calendering improved gloss compared to soft nip. Gloss of paper and print varied as: low Tg Styrene-Butadiene (SB) latex: High paper gloss & good print gloss, high Tg SB: low paper gloss, Styrene Acrylate (SA) latex: good paper and print gloss, Poly(vinyl acetate) (PVAc): Low paper and print gloss.
[153]	GCC + Kaolin	Calendering conditions	Calendering at lower temperature and higher line loads decreased light scattering of ability of coating and reduced gloss.

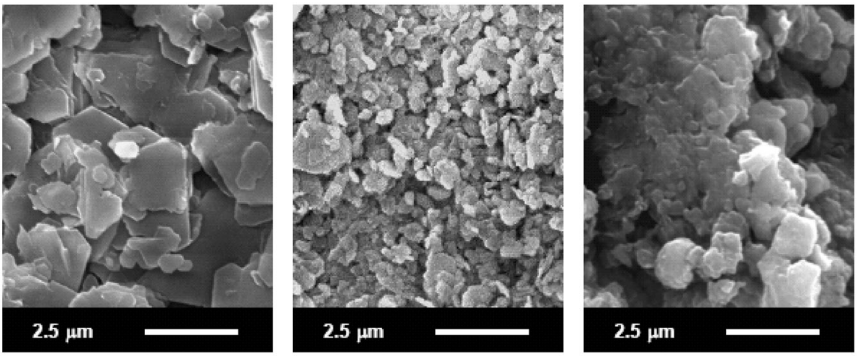

Figure 25. SEM micrographs of a) coarse clay with mean particle size: 2.16 µm;, b) fine clay with mean particle size: 0.26 µm, and c) ground calcium carbonate with mean particle size: : 0.77 µm [154].

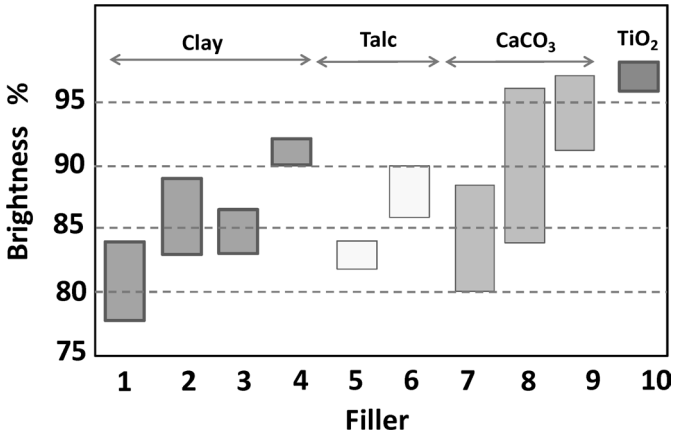

Figure 26. Brightness of common papermaking fillers. 1) European clay, 2) US clay, 3) US delaminated clay, 4) US calcined clay, 5) European talc, 6) Chinese talc, 7) European chalk, 8) GCC, 9) PCC, and 10) TiO_2 [130].

characteristics and pore structure of the coating/paper. Table 7 and Table 8 provide typical values of the light scattering coefficient and the refractive index for common fillers used in the paper industry.

KM theory may be used to estimate the scattering efficiency – and hence

Table 7. Light scattering coefficient of common fillers and virgin pulps [155].

Material	*Light Scattering Coeff. (m^2/kg)*	*Material*	*Light Scattering Coeff. (m^2/kg)*
Kaolin hydrous	70–120	Titanium dioxide	450–650
GCC	140–190	Silicate/silica	280–340
PCC	210–270	Chemical pulp	20–45
Calcined clay	200–300	Mechanical pulp	50–70

Table 8. Physical characteristics of coating pigments [156, 157].

Pigment	*Size (μm)*	*Shape*	*Density (kg/m^3)*	*Refractive Index*	*ISO Brightness*
Kaolin clay	0.3–5	Hexagonal platy	2.58	1.56	80–90
GCC	0.7–2	Cubic, prismatic, platy	2.7	1.56–1.65	87–97
PCC	0.1–1.0	Usually rod-like	2.7	1.59	96–99
Talcum	0.3–5	Platy	2.7	1.57	85–90
Gypsum	0.2–2	Roundish	2.3	1.52	92–94
Plastic pigments					
-Solid	0.1–0.5	Spherical	1.05	1.59	93–94
-Hollow	0.4–1.0	Spherical	0.6–0.9	1.59	93–94
Calcined kaolin	0.7 (median)	Aggregated plates	2.69	1.56	93
Titanium dioxide					
-Anatase	0.2–0.5	Rod-like	3.9	2.55	98–99
-Rutile	0.2–0.5	Roundish	4.2	2.70	98–99
Aluminum trihydrate	0.2–2	Platy	2.42	1.57	98–100

opacity and brightness – of filled and coated papers. In the case of filled papers, the additivity rule may be applied to determine the effective scattering and absorption coefficients [158]:

$$S\,W = S_1\,W_1 + S_2\,W_2 + \ \ldots \tag{75}$$

$$K\,W = K_1\,W_1 + K_2\,W_2 + \ \ldots \tag{76}$$

For coated papers, the layered model described by Equations (16) to (18) can be used. In practice, the reflectance of a single sheet of coated paper, $R_{o,12}$, may be obtained without any transmittance measurements using:

$$R_{o,12} = \frac{(R_{o,1} - R_{\infty,1})/R_{\infty,1} - R_{\infty,1}\,(R_{o,2} - 1/R_{\infty,1}) \exp\left(2\,S_1\,W_1\left(\frac{1}{R_{\infty,1}} - R_{\infty,1}\right)\right)}{(R_{o,2} - R_{\infty,1}) - (R_{o,2} - 1/R_{\infty,1})\,\exp\left(2\,S_1\,W_1\left(\frac{1}{R_{\infty,1}} - R_{\infty,1}\right)\right)} \quad (77)$$

Based on the above approach, the reflectance and scattering of the coating layer can be estimated based on the measurement of reflectance values of coated papers with two different backings [139, 159]:

$$R_{\infty,c} = \frac{c - \sqrt{c^2 - 4}}{2}$$

where :

$$c = \frac{(R_{g1} + R_2)\left(R_1\,R_{g2} - 1\right) - \left(R_{g2} + R_1\right)(R_2\,R_{g1} - 1)}{R_1\,R_{g2} - R_2\,R_{g1}}$$

Here, $R_{\infty,c}$ is the reflectance of an infinitely thick coating layer, R_1 and R_2 are the reflectances of a single sheet of coated paper with different backings ($R_1 < R_2$), R_{g1} is the reflectance of substrate 1 (black cavity), and R_{g2} is the reflectance of substrate 2 (a sufficiently large number of sheets of base paper). Using this method, Hamada *et al.* found a linear relationship between the light scattering coefficient and brightness of coating layer (i.e. $R_{\infty,c}$). Experimental studies have shown that the scattering coefficient and reflectance of coating layer determined in this way depend on the binder content, degree of calendering, and the base sheet properties. In particular, a non-absorptive base sheet is known to have a substantially lower scattering coefficient [159].

As discussed earlier, KM theory is an approximation of the more general radiative transfer model, and the absorption and scattering coefficients in KM theory, K and S, are not material properties. Instead, these coefficients should be regarded as model parameters that fit the experimental observations for a given set of materials. However, it would be advantageous to predict the scattering efficiency of filled papers and coating layers based on characteristic of paper constituents, i.e. fibres, fillers, and pigments. This could be addressed by resorting to theories that describe light-particle interaction.

The typical size of papermaking pigments is of the order of wavelength of light; hence, Mie theory may be applied to study the interaction of light with pigment particles. Based on Mie theory, scattering and absorption of a particle depend on particle size, dielectric properties, and the wavelength of incident light [29, 30]. This theory has been originally developed for light interaction with a single particle; however, it may be also used for loosely packed particle systems [160]. Mie theory has been applied in combination with the KM model to estimate the optical properties of coatings, paints and polymer films. For dilute particle systems, where inter-particle interactions may be ignored, KM absorption and scattering coefficients may be estimated based on the Mie's absorption and scattering cross sections of a single pigment particle and by using Equations (30) and (31). Although paints and coatings are densely packed systems, this approximation has been often used to examine the relative changes of K and S with variations in pigment characteristics [161].

To account for particle interactions in densely packed systems, various corrections have been proposed to improve the predictions of Mie theory [162–166]. Based on Van de Hulst's approach, Brinkworth assumed that the scattering cross section of a suspension of monodispersed spherical particles can be expressed in terms of the volume concentration of particles V_p, particle diameter D, and the scattering efficiency of a single particle Q_{sca} [166]:

$$\sigma_s = \frac{3}{2}\frac{Q_{sca}}{D}(1 - \mathrm{g})\,V_p \tag{78}$$

where g is the asymmetry factor that is defined as the average cosine of the scattering angle (see Equation (21)). If the incident energy were totally forward scattered then $g = +1$, but if it were fully backscattered, then $g = -1$. Scattering efficiency is the ratio of the scattering cross section and the geometrical cross section of the particle (i.e. $4\sigma_s / \pi D^2$). For cases where the refractive index of particle is close to that of medium, the scattering efficiency is given by [166]:

$$Q_{sca} = (\varepsilon_r - 1)^2\,\Phi(D, \lambda) \tag{79}$$

where ε_r is the ratio of the refractive index of the particle to that of the surroundings.

Using an approach similar to Brinkworth and by implementing Gate's equation for scattering cross section (Equation (20)), Ross proposed the following model that takes into account the volume concentration of particles, anisotropy of the scattered field, and illumination conditions [163]:

$$S = \frac{9}{8}\, c\,(1-g)\,\frac{Q_{sca}}{D}\, V_p \tag{80}$$

The parameter c in the above equation is a constant that depends on the illumination geometry and surface reflection effects. Assuming that there is no boundary surface to complicate the path of light by refraction and reflection, i.e. pigment particles are dispersed in air, two cases were considered: diffuse illumination for which $c = 1$, and normal collimated illumination for which $c = 0.8$. Note that S has the unit of inverse length. Using Ross' model, Borch and Lepoutre estimated the variations in the light scattering coefficients of coatings containing spherical pigments as a function of pigment size and refractive index [167].

Strictly speaking, neither KM nor Mie theory are suitable for the prediction of optical properties of paper coatings because: 1) pigment size is close to the optical wavelengths of light, and 2) packing density of typical coatings is above 50% while Mie theory and RTE are only applicable for low packing densities (<10%). It is well-known that a high concentration of pigment particles results in inter-particle interactions and reduces the overall scattering efficiency [164]. To address this problem, various analytical and numerical methods have been suggested that do not suffer from the limitations of Mie and KM theories. In particular, an elegant extension of Mie theory has been suggested by Flesia and Schwendimann to account for multiple scattering effects [31]. Others have resorted to numerical solutions to study the crowding and particle-particle interaction effects at higher pigment volume concentrations. Figure 27 shows one such simulation that illustrates the near field scattering for two adjacent titanium dioxide particles in a polymer matrix based on the finite element solution to Maxwell's equation [168]. The far field scattering coefficient of these two particles reduced from ~24 μm^{-1} to about 22 μm^{-1} as particle-particle separation decreased from 500 nm to zero.

More recently, Penttilä *et al.* applied the discrete dipole approximation (DDA) to predict the reflectance and transmittance of densely packed coating layers [169]. DDA is an approximate solution to the Maxwell equations for studying the scattering and absorption of radiation by particles with arbitrary geometry. It is based on partitioning the medium into small polarized cells called dipoles that acquire dipole moments in response to the local electric field [170]. Using DDA it is possible to account for changes in scattering efficiency of the coating layer due to variations in the packing density and pigment characteristics; such as size, shape, and refractive index. This is a useful approach that helps to design better pigments with enhanced optical performance by optimizing size, geometry, and refractive index. Based on this method, Penttilä *et al.* studied the scattering coefficient, reflectivity and

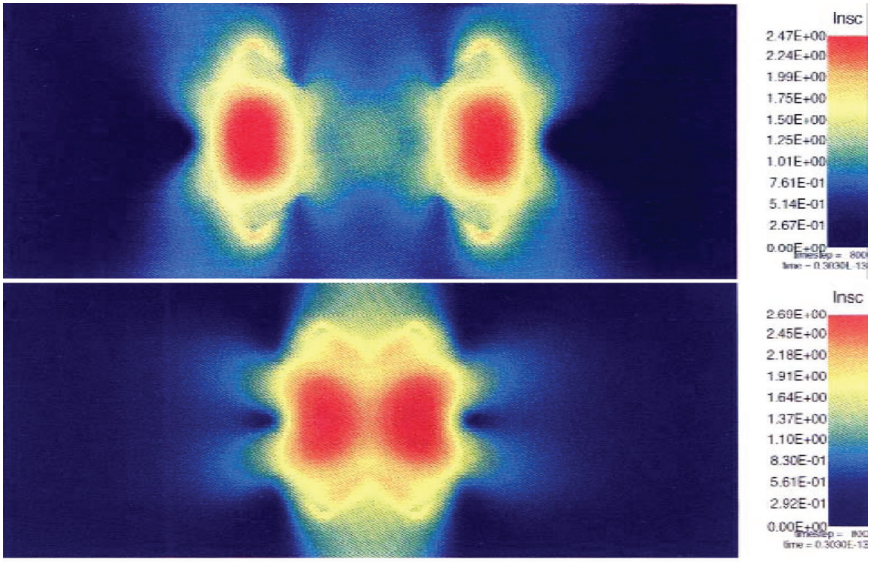

Figure 27. Simulated near field scattering for two anisotropic rutile titanium dioxide particles in a resin with n = 1.514. Particle-particle distances are 0.2 μm (top) and 0 (bottom), incident light is normal to the surface of paper and wavelength of light is 560 nm [168].

transmittance of model coating layers composed of starch acetate pigments as a function of packing density and pigment particle size (Figure 28.a). They found that at a refractive index of 1.47, the scattering coefficient decreased from ~10 μm^{-1} for a 0.2 μm pigment to a minimum value of 6.5 μm^{-1} for a pigment size of about 0.7–0.8 μm (Figure 28.b). In contrast, at n = 1.67 (not shown here), the light scattering coefficient increased slightly before decreasing at above a pigment size of 0.5 μm. This approach is currently being extended to predict the effects of pigment modification on the optical properties of coatings [171].

In practice, the reduction in the scattering coefficient caused by pigment particle interactions is detrimental to the optical properties of coating layers. Figure 29 illustrates the effect of volume concentration of titanium dioxide on the KM scattering coefficient. It is evident that by increasing TiO_2 concentration beyond ~25 v/v%, there is little gain in the scattering ability of the coating [164]. Such effects, however, may be negated by the introduction of a co-pigment [172, 173].

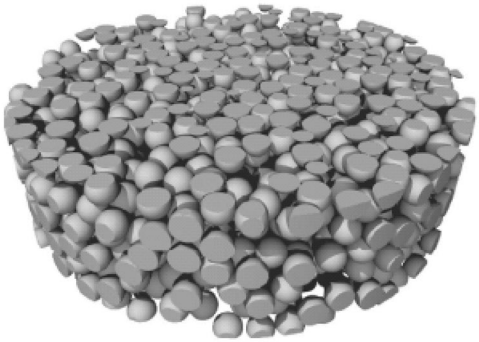

(a)

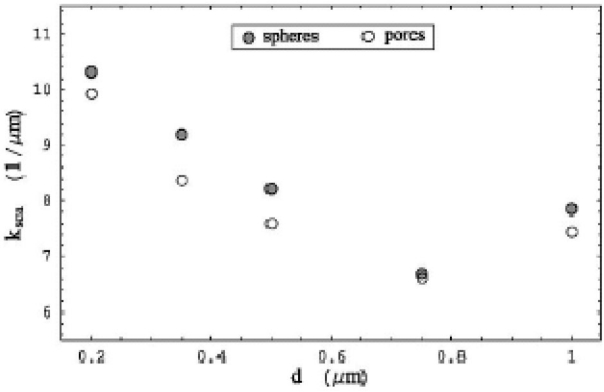

(b)

Figure 28. (a) A model cylindrical coating structure containing 1400 pigment particles with a packing density of ~50%, and (b) the predicted light scattering coefficient of the model coating layer [169].

An alternative method to enhance light scattering of coating layers is to introduce microvoids into the coating's structure. It has long been known that microvoids are able to increase the "hiding" power of coatings and paints. Ross reported that the theoretical light scattering coefficient of micro-bubbles in a latex resin is about 12% of that of rutile titanium dioxide (Figure 30) [163]. In an experimental study concerning latex coatings, Pierce *et al.* found that microvoids have a scattering coefficient of about 0.064 to 0.070 μm^{-1} [174]. Furthermore, they reported that it is possible to achieve the same overall scattering coefficient by introducing microvoids and significantly reducing

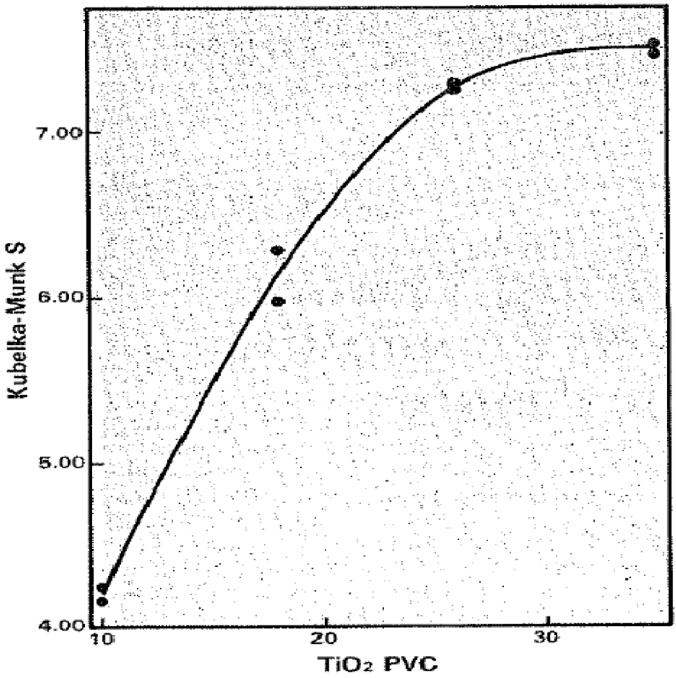

Figure 29. Effect of pigment volume concentration on the KM scattering coefficient for titanium dioxide [164].

the amount of TiO_2. Most recently, using the numerical model described earlier, Penttilä *et al.* investigated starch acetate coating layers containing microvoids and found that the scattering coefficient of these layers decreased from 10 μm^{-1} to about 7 μm^{-1} as the void diameter increased from 200 nm to 800 nm (Figure 28.b). These values, however, are significantly higher than the experimental values of Pierce *et al.* and theoretical predictions of Ross.

One way to introduce "voids" in coating structure is through the addition of hollow pigments. Hollow plastic pigments are commonly used to improve the optical performance of the coating layer, the coated paper's reflectance and its gloss [139, 175, 176]. Recently, Enomae and Tsujino demonstrated that similar improvements may be realized by introducing hollow inorganic pigments into the coating formulations. They synthesized hollow calcium carbonate pigments with a primary particle size of 50 nm and examined their performance both as filler and as coating pigment [177]. They observed a positive effect on the coating brightness and light scattering coefficient.

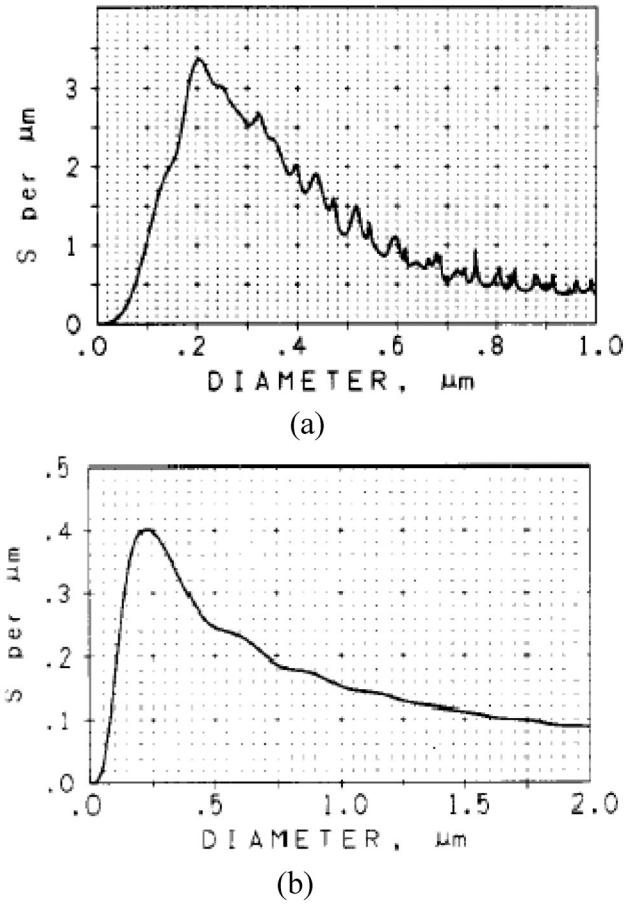

Figure 30. Theoretical KM scattering coefficients of uniform spherical rutile pigments in resin (a) and spherical microvoids in resin (b) as a function of sphere diameter [161].

CONCLUDING REMARKS

Significant progress has been made in our understanding of the interaction of light with paper and its effect on paper's appearance. Advancements in computers, digital imaging, and laser light sources have resulted in the development of a variety of modern instrumental assemblies to examine the optical properties of paper in novel ways, at speeds that were not possible a few years

ago. These advancements have enabled us to map optical properties of paper at a high resolution over relatively large areas. This is advantageous since our perception of paper quality is not only affected by the average values of optical characteristics of paper but also by their local variations at relatively small scales, i.e. at the scale of fibre length and below. However, despite these technological advancements, typical standard testing methods only provide "average" measurements of optical properties over relatively large areas. Development of standardized methods that take advantage of these advancements would be beneficial not only to practitioners but also to researchers in this field.

Progress in our theoretical understanding of propagation and surface scattering of waves in random media driven by remote sensing, material testing, and medical imaging applications, has provided us with new insights into the relationship between paper's structure and its optical properties. In spite of this progress, our quest for developing physical models to predict the optical properties of paper based on its structure and furnish characteristics is still ongoing. Numerical simulations of light-paper interaction, similar to those discussed in this article, offer a promising possibility to achieve this goal. However, further work is required to improve these models while taking into account the effects of base sheet and coating structure, as well as fibre and pigment characteristics.

The surface structure of paper plays an important role in terms of its optical properties, especially gloss. Today, confocal laser scanning microscopy, atomic force microscopy, and a variety of surface topography measurement techniques are available to characterize paper surface structure at high resolutions. However, we still lack a fundamental understanding of effect of paper furnish, forming and finishing conditions on paper surface statistics. This is further complicated by the fact that rms roughness and correlation length of surface heights depend both on the sample size and measurement resolution. Further fundamental work is required to better understand these effects.

With escalating cost and reduced availability of fibre resources, there is an increasing desire to increase the amount of filler and/or reduce grammage of paper, while maintaining adequate optical properties for printing and writing papers. On the other hand, rapid growth of digital printing technology has introduced new demands on the paper performance and characteristics. These competing factors stress the need for a better fundamental understanding of the relationships among structure, furnish, and optical properties of paper.

Over the next decade, rapid reduction in the consumption of printing and writing papers in mature market regions, such as North America, combined

with increased environmental awareness, will likely transform the face of pulp and paper industry as we know it. The emergence of novel green paper-based products for new applications that take advantage of wood fibres as a biodegradable and renewable resource is imminent. Inevitably, these new products will impose different demands and new challenges in terms of the optical properties of paper, but they also present us with an opportunity to further improve our fundamental understanding of these properties and to contribute to the advancement of optical science and technology.

ACKNOWLEDGEMENTS

The author wishes to thank Mr. Duoyin Lu for his help with the literature search and Mr. Peter Angelo for his editing work on this document.

REFERENCES

1. PAPTAC Standard E.1. Brightness of Pulp, Paper, and Paperboard. In *Pulp and Paper Technical Association of Canada Standard Testing Methods*, 1990.
2. J.A. Bristow. What Is ISO Brightness? *TAPPI J.* 77(5):174–178, 1994.
3. B.D. Jordan and M.A. O'neill. The Whiteness of Paper- Caolorimetry and Visual Ranking. *TAPPI J.* 74(5) 1991.
4. J.A. Bristow and C. Karipidis. ISO Brightness of Fluorescent Papers and Indoor Whiteness-Proposal for Illuminant. *TAPPI J.* 82(1):183–193, 1999.
5. S.J. Popson, D.D. Malthouse and R.C. Robertson. Applying Brightness, Whiteness, and Color Measurements to Color Removal. *Tappi J.* 80(9):137–147, 1997.
6. PAPTAC Standard E.2. Opacity of Paper. In *Pulp and Paper Technical Association of Canada Standard Methods*, 1993.
7. R. Silvennoinen, K.-E. Peiponen and K. Myller. Traditional Glossmeters. Ch.7 in **Specular Gloss**, pp. 267–314, Elsevier, Amsterdam, 2008b.
8. J. Borch. Optical and Appearance Properties. Ch.4 in **Handbook of Physical Testing of Paper**, vol. 2, (ed. R.E. Mark, M.B., Lyne and J. Borch), pp. 95–148, Marcel Dekker, New York, 2002.
9. M. Leskelä. Optical Properties. Ch. 4 in **Paper Physics**, (ed. K. Niskanen), pp. 117–137, Finish Paper Engineers' Association and Tappi Press, Helsinki, 1998.
10. L.T. Sharpe, A. Stockman, W. Jagla and H. Jagle. A Luminous Efficiency Function, V*(), for Daylight Adaptation. *J. Vision* 5(11):577–585, 2005.
11. A. Stockman and L.T. Sharpe. The Spectral Sensitivities of the Middle- and Long-Wavelength-Sensitive Cones Derived from Measurements in Observers of Known Genotype. *Vision Res.* 40(13):1711–1737, 2000.
12. M. Baneshi, S. Maruyama, H. Nakai and A. Komiya. A New Approach to

Optimizing Pigmented Coatings Considering Both Thermal and Aesthetic Effects. *J. Quant. Spectrosc. Radiat. Transfer* 110(3):192–204, 2009.
13. X. Hu and K.W. Houser. Spectral and Electrical Performance of Screw-Based Dimmable Cmpact Fluorescent Lamps. *Lighting Res. Technol.* 35(4):331–342, 2003.
14. P. Hansson. Simulation of Small Scale Print Gloss Variations Based on Topographic Data. *NPPRJ* 19(1):112–115, 2004.
15. M. Lindstrand. An Angularly and Spatially Resolved Reflectometry for a Perceptually Adequate Characterization of Gloss. *JIST* 49(1):71–84, 2005.
16. J.S. Arney, P.G. Anderson, G. Franz and W. Pfeister. Color Properties of Specular Reflections. *JIST* 50(3):228–232, 2006.
17. J.S. Arney and D. Nilosek. Analysis of Print Gloss with a Calibrated Microgoniophotometer. *JIST* 51(6):509–513, 2007.
18. G. Bernard, R. Farnood and N. Yan. Customized Setup to Assess Microgloss Uniformity of Paper. *Pulp & Paper Can.* 106(9):T190–193, 2005.
19. M.A. Macgregor and P.-A. Johansson. Submillimeter Gloss Variations in Coated Paper: Part I. The Gloss Imaging Equipment and Analytical Techniques. *Tappi J.* 73(12):161–168, 1990.
20. N.J. Elton and J.S. Preston. Polarized Light Reflectometry for Studies of Paper Coating Structure. Part I. Method and Instrumentation. *Tappi J.* 5(7):8–16, 2006.
21. Y.-J. Sung and D.S. Keller. Evaluation of Gloss Variation with a Novel Method. *J. Korea Tappi* 34(2):73–83, 2002.
22. M. Sorjonen, A. Jääskeläinen, K.-E. Peiponen and R. Silvennoinen. On the Assessment of the Surface Quality of Black Print Paper by Use of a Diffractive Optical-Element-Based Sensor. *Meas. Sci. Technol.* 11(6):N85–N88, 2000.
23. J. Palviainen, M. Sorjonen, R. Silvennoinen and K.-E. Peiponnen. Optical Sensing of Colour Print on Paper by Diffractive Optical Element. *Meas. Sci. Technol.* 13(4):N31–N37, 2002.
24. R. Silvennoinen, *et al.* Diffractive Element in Optical Inspection of Paper. *Opt. Eng.* 37(5):1482–1487, 1998.
25. M. Juuti, V. Kalima, T.T. Pakkanen and K.-E. Peiponen. A Novel Method to Measure and Analyse Delta Gloss by Diffractive Glossmeter. *Meas. Sci. Technol.* 18(5):L5–L8, 2007.
26. M. Jutti, H. Koivula, M. Toivakka and K.-E. Peiponen. A Diffractive Gloss Meter for Local Gloss Measurements of Papers and Prints. *Tappi J.* 7(4):27–32, 2008.
27. A. Apostol, D. Haefner and A. Dogariu. Near-Field Characterization of Effective Optical Interfaces. *Physical Rev. E.* 74(6):066603, 2006.
28. D. Ma, R.D. Carter, D. Haefner and A. Dogariu. Simultaneous Characterization of Coated Paper Topography and Optical Contrast by near-Field Scanning Optical Microscopy (Nsom). *NPPRJ* 23(4):438–443, 2008.
29. A. Ishimaru. **Wave Propagation and Scattering in Random Media**, IEEE, New York 1997.

30. G. Mie. Contributions to the Optics of Turbid Media, Particularly of Colloidal Metal Solutions. *Annal. Phys.* 25(3):377–445, 1908.
31. C. Flesia and P. Schwendimann. Analytical Multiple Scattering Extension of the Mie Theory – Part I: General Discussion. *Appl. Phys. B* 56(3):157–163, 1993.
32. J.A. Ogilvy. **Theory of Wave Scattering from Random Rough Surfaces**, Bristol: Adam Hilger 1991.
33. A.K. Fung. **Microwave Scattering and Emission Models and Their Applications**, Artech House, Boston 1994.
34. O.M. Johannessen, V.Yu. Alexandrov, I.Ye. Frolov, S. Sandven, L.H. Pettersson and L.P. Bobylev. **Remote Sensing of Sea Ice in the Northern Sea Route**, Springer, Berlin 2007.
35. P. Beckmann and A. Spizzichino. **The Scattering of Electromagnetic Waves from Rough Surfaces**, Oxford: Pergamon, 1963.
36. G. Berginc. Small-Slope Approximation Method: A Further Study of Vector Wave Scattering from Two-Dimensional Surfaces and Comparison with Experimental Data. *PIER* 37(2002):251–287, 2002.
37. T.M. Elfouhaily and C.-A. Guérin. A Critical Survey of Approximate Scattering Wave Theories from Random Rough Surfaces. *Waves in Random Media* 14(4):R1–R40, 2004.
38. C.-A. Guérin, G. Soriano and T. Elfouhaily. Weighted Curvature Approximation: Numerical Tests for 2 D Dielectric Surfaces. *Waves in Random Media* 14(3):349–363, 2004.
39. K.F. Warnick and W.C. Chew. Numerical Simulation Methods for Rough Surface Scattering. *Waves Random Media* 11(1):R1–R30, 2001.
40. T.R. Lettieri, E. Marx, J.-F. Song and T.V. Vorburger. Light Scattering from Glossy Coatings on Paper. *Appl. Opt.* 30(30):4439–4447, 1991.
41. N. Dechamps and R. Farnood. Modeling of Paper Gloss Using Geometrical Optics Approximation. Pulp & Paper Centre Internal Report. University of Toronto, 2006.
42. P.S. Mudgett and L.W. Richards. Multiple Scattering Calculations for Technology. *Appl. Opt.* 10(7):1485–1502, 1971.
43. P. Kubelka. New Contributions to the Optics of Intensely Light-Scattering Materials. Part I. *J. Opt. Soc. Am.* 38(5):448–457, 1948.
44. L.F. Gate. Comparison of the Photon Diffusion Model and Kubelka-Munk Equation with the Exact Solution of the Radiative Transport Equation. *Appl. Opt.* 5(4):837–846, 1974.
45. J.-F. Bloch and R. Sève. About the Theoretical Aspect of Multiple Light Scattering: Silvy's Theory. *Color Res. Appl.* 28(3):227–228, 2003.
46. J. Silvy. Contribution À L'étude De La Diffusion Multiple De La Lumière Dans Le Cadre De L'approximation De Diffusion. *Rev. Opt., Theor. Instrum.* 40(10):495–517, 1961.
47. S.L. Jacques. Reflectance Spectroscopy with Optical Fibre Devices, and Transcutaneous Bilirubinometers. In **Biomedical Optical Instrumentation and**

Laser-Assisted Biotechnology, (ed. S.M. A.M. Verga Scheggi, A.N. Chester and R. Pratesi), pp. 83–94, Kluwer Academic, Boston, 1996.
48. S.N. Thennadil. Relationship between the Kubelka-Munk Scattering and Radiative Transfer Coefficients. *J. Opt. Soc. Am. A* 25(7):1480–1485, 2008.
49. B.J. Brinkworth. Interpretation of Kubelka-Munk Coefficient in Reflection Theory. *Appl. Opt.* 11(6):1434–1435, 1972b.
50. W.M. Star, J.P.A. Marijnissen and M.J.C. Van Gemert. Light Dosimetry in Optical Phantoms and in Tissues: I. Multiple Flux and Transport Theory. *Phys. Med. Biol.* 33(4):437–454, 1988.
51. A. Alince, J. Porubská and T.G.M. Van De Van. Light Scattering and Microscopy in Paper. *JPPS* 28(3):93–98, 2002.
52. L.K. Lehtonen and T.J. Dyer. Light-Scattering Coefficient as a Measure of Specific Surface Area in Mechanical Pulp Laboratory Sheets. *Paperi ja puu* 87(8):517–524, 2005.
53. W.J. Foote. Investigation of Fundamental Scattering and Absorption Coefficients of Dyed Handsheets. *Paper Trade J.* 109(25):31–38, 1939.
54. L. Nordman, P. Aaltonen and T. Makkonen. Relationship between Mechanical and Optical Properties of Paper Affected by Web Consolidation. In *Transactions of the Symposium on Consolidation of the Paper Web*, pp. 909–927. Cambridge: Tech. Section British Paper and Board Makers' Assoc., London, 1996.
55. A.A. Koukoulas and B.D. Jordan. Effect of Strong Absorption on the Kubelka-Munk Scattering Coefficient. *JPPS* 23(5):J224–232, 1997.
56. P. Edstrom. Comparison of the Dort2002 Radiative Transfer Solution Method and the Kubelka-Munk Model. *NPPRJ* 19(3):397–403, 2004.
57. H. Granberg, M. Rundlöf and L. Mattsson. Influence of Surface-Induced Non-uniform Reflectance on the Diffuse Reflectance Factor. Part I: Model Predictions. *JPPS* 29(8):247–253, 2003.
58. L. Yang and B. Kruse. Revised Kubelka-Munk Theory: I. Theory and Application. *J. Opt. Soc. Am. A* 21(10):1934–1942, 2004.
59. A. Mandelis and J.P. Grossman. Perturbation Theoretical Approach to the Generalized Kubleka-Munk Problem in Nonhomogeneous Optical Media. *Appl. Spectrosc.* 46(5):737–745, 1992.
60. L.F. Gate. The Determination of Light Absorption in Diffusing Materials by a Photon Diffusion Model. *J. Phys. D: Appl. Phys.* 4(7):1049–1056, 1971.
61. B. Philips-Invernizzi, D. Dupont and C. Caze. Bibliographical Review for Reflectance of Diffusing Media. *Opt. Eng.* 40(5):1082–1092, 2001.
62. E. Ganz. Whiteness: Photometric Specification and Colorimetric Evaluation. *Appl. Opt.* 15(9):2039–2058, 1976.
63. PAPTAC Standard E.5. Pulp, Paper and Paperboard- Colour Measurement with a Diffuse/Zero Geometry Tristimulus Reflectometer. In *Pulp and Paper Technical Association of Canada Standard Methods*, 1993.
64. J.S. Bonham. The Appearance of 'White' Papers. *Appita J.* 50(6):446–451, 2006.
65. H. Liu, S. Yang and Y. Ni. Using Dyes for Improving the Optical Properties of High Yield Pulps. *Pulp & Paper Canada* 108(10):T157–160, 2007.

66. E. Milanova and B.B. Sithole. A Simple Method for Estimation of Newsprint Dyes in Effluents and Their Migration from Paper Samples. *Tappi J.* 80(5):121–128, 1997.
67. L. Cabos, M. Berrada and J. Paris. Effect of Furnish Composition on the Color of a Fine Three-Ply Paperboard. *Tappi J.* 83(10):1–16, 2000.
68. B. Aksoy, M.K. Joyce and P.D. Fleming. Comparative Study of Brightness/ Whiteness Using Various Analytical Methods on Caoted Papers Containg Colorants. In *TAPPI Spring Technical Conference and Exhibit*, pp. 371–385, Chicago, IL. Technical Association of Pulp and Paper Industry, Atlanta, 2003.
69. M.O.A. Mäkinen, T. Jääkelainen and J. Parkkinen. Improving Optical Properties of Printing Papers with Dyes: A Theoretical Study. *NPPRJ* 22(2):236–243, 2007.
70. A.V. Makarenko and I.A. Shaykevich. Dependence of the Whiteness of Paper on Surface Roughness and Illumination Conditions. *Color Res. Appl.* 25(3):170–175, 2000.
71. W.J. Auhorn. Chemical Additives. Ch. 3 in **Handbook of Paper and Board**, (ed. H. Holik), pp. 62–149, Wiley-VCH Verlag, 2006.
72. O. Jokinen, R. Baak, G. Traser and P. Rohringer. Optical Brighteners for High White Coated Paper. *Wochenblatt für Papierfabrikation* 128(9):590–593, 2000.
73. J.-E.P. Nordström, J.P. Nordlund and J.P.L. Grön. Effect of Optical Brightening Agents Degradation Due to Heat and Moisture- Determining Optical Mottle? *Paperi Ja Puu* 80(6):449–458, 1998.
74. M. Cieplinski and E. Drzewinska. The Effect of Fluorescent Whitening Agents and Tinting Dyes on Permanence of Paper Colour. *Paper Technol.* 48(5):37–40, 2007.
75. D. Ma, R.D. Carter, D. Haefner and A. Dogariu. The Influence of Fine Kaolin and Ground Calcium Carbonates on the Efficiency and Distribution of Fluorescence Whitening Agents (Fwa) in Paper Coating. *NPPRJ* 23(3):327–332, 2008.
76. J.S. Bonham. Fluorescence and Kubelka-Munk Theory. *Color Res. Appl.* 11(3):223–230, 1985.
77. Y.Y. Kulikova, M.K. Schaepe and W.B. Robbins. Assessment of the Influence of Paper Formation on the Fluorescence Contribution to Brightness. *Color Res. Appl.* 20(2):87–92, 1995.
78. B.T. Hallam and A.G. Hiorns. Developing Optical Efficiency through Optimised Coating Structure. In *Tappi Advanced Coating Fundamental Symposium Proceedings*, pp. 330–339, Turku. 2008.
79. Z. Yuan, J. Schmidt, C. Heitner and X. Zou. Coating Improves the Brightness Stability of Wood-Free Coated Papers Containing High-Yield Pulp. *Tappi J.* 5(1):9–13, 2006.
80. W.J. Hillend. Opacity Problems in Printing Papers: Kubelka-Munk Theory Gives Good, Quick Answers. *Tappi J.* 49(7):41A–47A, 1966.
81. M.O.A. Mäkinen, J. Parkkinen and T. Jääskeläinen. Generalized Opacity Basedx on Cielab Colour Coordinates and the CIE94 Colour Difference Formula. *JPPS* 31(1):61–67, 2005.

82. ISO2471. Determination of Opacity (Paper Backing)- Diffuse Reflectance Method. Geneva, Switzerland, 1998.
83. A. Dogariu and G.D. Boreman. Facet Model for Photon-Flux Transmission through Rough Dielectric Interfaces. *Opt. Let.* 21(10):701–703, 1996.
84. M.E. Nadal and E.A. Thompson. New Primary Standard for Specular Gloss Measurements. *J. Coatings Technol.* 72(911):61–66, 2000.
85. L.F. Gate, W. Windle and M. Hine. The Relationship between Gloss and Surface Microtexture of Coatings. *Tappi J.* 56(3):61–65, 1973.
86. P. Oittinen. The Surface Structure of Coated Paper and the Formation of Gloss. In *The Role of Fundamental Research in Paper Making. Transactions of the 7th Fundamental Research Symposium*, (ed. J. Brander), pp. 635–654, Cambridge. Mechanical Engineering Publications Ltd., 1981.
87. H. Lipschitz, M. Bridger and G. Derman. Relationships between Topography and Gloss. *TAPPI J.* 73(10):237–245, 1990.
88. M.A. Macgregor, P.-Å.. Johansson and M.-C. Béland. Measurement of Small-Scale Gloss Variation in Printed Paper: Topography Explains Much of the Variation for One Paper. In *International Printing and Graphic Arts Conference*, pp. 33–43, Haplifax. 1994.
89. M.-C. Béland, S. Lindberg and P.-Å. Johansson. Optical Measurement and Perception of Gloss Quality of Printed Matte-Coated Paper. *JPPS* 26(3):120–123, 2000.
90. G. Chinga. Detailed Characterization of Paper Surface Structure for Gloss Assessment. *JPPS* 30(8):222–227, 2004.
91. G. Chinga, P. O. Johnsen, R. Dougherty, E.L. Berli and J. Walter. Quantification of the 3D Microstructure of SC Surfaces. *J. Microsc.* 227(3):254–265, 2007.
92. N.J. Elton and J.S. Preston. Polarized Light Reflectometry for Studies of Paper Coating Structure. Part II. Application to Coating Structure, Gloss and Porosity. *Tappi J.* 5(8):10–16, 2006.
93. R. Alexander-Katz and R.G. Barrera. Surface Correlation Effects on Gloss. *J. Polymer Sci. B* 36(8):1321–1334, 1998.
94. E. Caner, R. Farnood and N. Yan. Relationship between Gloss and Surface Texture of Coated Papers. *TAPPI J.* 7(4):19–26, 2008.
95. P. Vernhes. Relevant Paper Properties for Digital Printing, Ph.D. Thesis, Ecole internationale du papier, de la communication imprimée et des biomatériaux, Grenoble, 2008.
96. P. Vernhes, J.F. Bloch, C. Mercier, A. Blayo and B. Pineaux. Statistical Analysis of Paper Surface Microstructure: A Multi-Scale Approach. *Appl. Surf. Sci.* 254(22):7431–7437, 2008.
97. P. Vernhes, J.-F. Bloch, A. Blayo and B. Pineaux. Gloss Optical Elementary Representative Surface. *Appl. Opt.* 47(29):5429–5438, 2008.
98. K. Green, L. Lamberg and K. Lumme. Stochastic Modeling of Paper Structure and Monte Carlo Simulation of Light Scattering. *Appl. Opt.* 39(25):4669–4683, 2000.
99. R. Farnood and N. Dechamps. Use of Recent Electromagnetic Theories to

Predict Paper Gloss and Microgloss Nonuniformity. Pulp & Paper Centre Internal Report, University of Toronto, 2005.
100. J.S. Arney, L. Ye and S. Banach. Interpretation of Gloss Meter Measurements. *JIST* 50(6):567–571, 2006.
101. C. Bourlier and G. Berginc. Multiple Scattering in the High-Frequency Limit with Second Order Shadowing Function from 2D Anisotropic Rough Dielectric Surfaces: I. Theoretical Study. *Waves in Random Media* 14(3):229–252, 2004.
102. V.I. Tatarskii and W.V. Tatarskii. Statistical Description of Rough-Surface Scattering Using the Quasi-Small-Slope Approximation for Random Surfaces with a Gaussian Multivariate Probability Distribution. *Waves Random Complex Media* 4(2):191–214, 1994.
103. J. Järnström, L. Sinervo, M. Toivakka and J. Peltonen. Topography and Gloss of Precipitated Calcium Carbonate Coating Layers on a Model Substrate. *Tappi J.* 6(5):23–31, 2007.
104. J.A. Van Den Akker. Optical Properties of Paper. In **The Structure and Physical Properties of Paper**, (ed. H.F. Rance), pp. 127–174, Elsevier, Amsterdam, 1982.
105. R.M. Leekley, C.W. Denzer and R.F. Tyler. Measurement of Surface Reflection from Paper and Prints. *Tappi J.* 53(4):615–621, 1970.
106. J.S. Arney, L. Ye, J. Wible and T. Oswald. Analysis of Paper Gloss. *JPPS* 32(1):19–23, 2006.
107. T. Takahashi and R. Farnood. Contribution of Surface and Bulk Scattering to the Gloss of Coated Papers. In *Tappi Coating Conference*, Salt Lake City. TAPPI Press, Atlanta, 2009.
108. T. Glatter and D.W. Bousefield. Print Gloss Development on a Model Substrate. *Tappi J.* 80(7):125–132, 1997.
109. J.S. Preston, G.C. Allen, J.J. Elton, J.C. Husband, J.S. Dalton and P.J. Heard. Investigation into the Distribution of Ink Components Throughout Printed Coated Paper- Part1: Optical and Roughness Considerations. *Colloids Surf. A* 205(3):183–198, 2002.
110. M.A. Macgregor and P.-Å. Johansson. Gloss Uniformity in Coated Paper. In *Tappi Coating Conference*, pp. 495–504, Montreal. Tappi Press, Atlanta, 1991.
111. G. Ström, A. Englund and M. Karathanasis. Effect of Coating Structure on Print Gloss after Sheet-Fed Offset Printing. *NPPRJ* 18(1):108–115, 2003.
112. D.W. Donigian, J.N. Ishley and K.J. Wise. Coating Pore Structure and Offset Printed Gloss. *Tappi J.* 80(5):163–172, 1997.
113. Y. Arai and K. Nojima. Coating Structure for Obtaining High Print Gloss. *Tappi J.* 81(5):213–221, 1998.
114. J.S. Preston, D.J. Parsons, J.C. Husband and C. Nutbeen. Ink Gloss Development Mechanisms after Printing. Part 2-the Influence of Substrate. In *Advanced Coating Fundamentals Symposium*, Chicago. TAPPI Press, Atlanta, 2003.
115. N. Matsuda, T. Ichihashi and Y. Zama. Influence of Ultrafine Surface Profile to Sheet and Print Gloss of Coated Paper. *Japan Tappi J.* 54(4):25–33, 2000.
116. G. Ström and M. Karathanasis. Relationship between Ink Film Topography and Print Gloss in Offset Prints on Coated Surfaces. *NPPRJ* 23(2):156–163, 2008.

117. E. Caner, R. Farnood and N. Yan. Effect of the Coating Formulation on the Microgloss Nonuniformity of Coated Papers. In *PAPTAC Annual Meeting*, pp. C9–C12, Montreal. Pulp and Paper Technical Association of Canada, Montreal, 2005.
118. H. Fujiwara, C. Kaga and I. Kano. Measurement of Gloss Profile. In *Tappi Coating Conference*, pp. 209–218, Boston. 1990.
119. M.-C. Béland and J.M. Bennett. Effect of Local Microroughness on the Gloss Uniformity of Printed Paper Surface. *Appl. Opt* 39(6):2719–2726, 2000.
120. M.A. Macgregor. A Review of the Topographical Causes of Gloss Variation and the Effect on Perceived Print Quality. In *Proceedings of the Hansol Research Symposium*, Seoul, Korea. 2000.
121. E. Caner, R. Farnood and N. Yan. Effect of the Coating Formulation on the Gloss Properties of Coated Papers. In *International Printing and Graphic Arts Conference*, Cincinnati. TAPPI Press, Atlanta, 2006.
122. M.A. Hubbe, J.J. Pawlak and A.A. Koukoulas. Paper's Appearance: A Review. *bioresources* 3(2):627–665, 2008.
123. R. Bown. A Review of the Influence of Pigments on Papermaking and Coating. In *The Fundamentals of Papermaking Materials. Transactions of the 11th Fundamental Research Symposium*, (ed. C.F. Baker), pp. 83–137, Cambridge. Pira International, Leatherhead, 1997.
124. H.V. Green, T.J. Fox and A.M. Scallan. Lumen-Loaded Paper Pulp. *Pulp Paper Can.* 83(7):39–43, 1982.
125. S.R. Middleton, J. Desmeules and A.M. Scallan. Lumen Loading with Calcium Carbonate Fillers. *JPPS* 29(7):241–246, 2003.
126. M.L. Miller and D.C. Paliwal. The Effects of Lumen-Loading on Strength and Optical Peroperties of Paper. *JPPS* 11(3):84–88, 1985.
127. P. Burri. **Properties and Performance Attributes between Coated Papers in North America, Europe, and Asia**, TAPPI Press, Toronto 2005.
128. H.H. Murray. Engineered Clay Products for the Paper Industry. *Appl. Clay Sci.* 29(3):199–206, 2005.
129. R.W. Wygant, R.R. Iyer and D.O. Cummings. Glossing Properties of Engineered Kaolins. In *Tappi Coating Conference*, pp. 873–852, New Orleans. TAPPI Press, Atlanta, 1998.
130. M. Laufmann. Fillers for Paper-a Global View. In *Proceedings of the PTS-Seminar Wet End Operations-Vorgänge in der Siebpartie*, pp. 1–6, Munich. 1998.
131. M. Lorusso. Base Paper Coating Interatcion: The Importance of Filler Design. *Paper Technol.* 45(2):37–41, 2004.
132. H. Al-Tuaif. The Effect of Pigment Blends on the Structure and Chemistry of Pigmented Latex Coatings. *TAPPI J.* 5(8):24–30, 2006.
133. A.C. Dimmick. Influence of the Average Particle Size of Aragonitic Precipitated Calcium Carbonate on Coated Paper Properties. In *Tappi Spring Technical Conference*, pp. 1–12, Chicago. TAPPI Press, Atlanta, 2003.
134. A.C. Dimmick. Effect of Sheet Moisture and Calendering Pressure on Pcc and Gcc Coated Papers. *Tappi J.* 6(10):16–22, 2007.

135. I. Endres and M. Tietz. Blade, Film and Curtain Coating Techniques and Their Influence on Paper Surface Characteristics. *Tappi J.* 6(11):24–32, 2007.
136. J. Hocken and M. Stefan. Titanium Dioxide and Zinc Sulphide: High-Quality Pigments for Special Papers. *Paper Technol.* 49(2):31–38, 2007.
137. A. Hedman, J. Gron and M. Rigdahl. Coating Layer Uniformity as Affected by Base Paper Characteristics and Coating Method. *NPPRJ* 18(3):333–343, 2003.
138. E. Caner, C. Quijano-Solis, R. Farnood and N. Yan. Multivariate Analysis of Micro-Gloss of Coated Papers. In *TAPPI Coating Conference*, Miami. TAPPI Press, Atlanta, 2007.
139. H. Hamada, T. Enomae, F. Onabe and Y. Siato. Characteristics of Hollow Sphere Plastic Pigment (Part I) -Optical Properties of Coated Paper and Colorimetric Control in Printing. *Jappan Tappi J.* 58(4):56–63, 2004.
140. A. Hiorns. Calendering Response of Calcium Carbonates in Doble Coated Woodfree Paper. In *Tappi Coating Conference*, pp. 127–146, Chicago. TAPPI Press, Atlanta, 2003.
141. J.C. Husband. Interactions between Ground Calcium Carbonate Pigments and Polymer Latices. *NPPRJ* 15(5):382–386, 2000.
142. L. Järnström, M. Wikström and M. Rigdahl. Porous Mineral Particles as Coating Pigments. *NPPRJ* 15(2):86–95, 2000.
143. H. Koyamoto and K. Okomori. Effect of Surface Properties of Base Paper on Print Quality. In *Advanced Coating Fundamentals Symposium*, pp. 217–227, Turku. TAPPI Press, Atlanta, 2006.
144. T. Lamminmäki, U. Forsstrom, M. Tienari, E. Saharinen, J. Mikkilä and J. Koskelainen. Calendering of Coated Paper at High Speeds and Temperatures. *NPPRJ* 20(3):354–360, 2005.
145. M. Larsson, G. Engström, D. Vidal and X. Zou. Impact of Calendering on Coating Structures. *NPPRJ* 22(2):267–274, 2007.
146. M. Larsson, D. Vidal, G. Engstrom and X. Zou. Paper Coating Properties as Affected by Pigment Blending and Calendering. *TAPPI J.* 6(8):16–22, 2007.
147. S. Lohmander. Influence of a Shape Factor of Pigment Particles on the Rheological Properties of Coating Colours. *NPPRJ* 15(3):231–136, 2000.
148. P.B. Malla, R.E. Starr, T.J. Werkin and S. Devisetti. Effects of Pigment Type and Pore Structure on Optical Properties and Rotogravure Printability of Light Weight Coated (Lwc) Paper – a Statistically Designed Clc Coating Study with Mixtures. In *Tappi Coating Conference*, pp. 407–430, San Diego. TAPPI Press, Atlanta, 2000.
149. Y.-S. Perng, I.-C. Wang, W.-C. Yang and M.-H. Lai. Application of Talc to Calcium Carbonate Containing Paper Coating Formulations. *Taiwan J. For. Sci.* 23(1):1–11, 2008.
150. J. Preston, A. Hiorns, D.J. Parsons and P. Heard. Design of Coating Structure for Flexographic Printing. *Paper Technology* 49(3):27–36, 2008.
151. Y. Wang and Z. Cao. Influence of Coating Pore Structure on Optical Properties of Low Gloss Coated Paper. In *TAPPI Advanced Coating Fundamentals Symposium*, pp. 276–285, Turku. TAPPI Press, Atlanta, 2006.

152. M. Wikström, M. Bouveng, J. Lindholm and J.-E. Teirfolk. The Influence of Different Coating Latices on Printing and Surface Properties of Paper Calendered at High Temperatures. *Wochenblatt für Papierfabrikation* 128(19):1321–1331, 2000.
153. M. Wikström, M. Bouveng, M. Rigdahl and A.G. Hiorns. Impact of High Temperature and Soft Nip Calendering on the Pore Structure of the Coating Layer. *NPPRJ* 17(2):147–152, 2000.
154. E. Caner. Effect of the Coating Formulation on the Microgloss and the Microgloss Nonuniformity of Coated Papers, M.A.Sc. Thesis, University of Toronto, 2006.
155. M. Laufmann. Pigments as Fillers. In **Handbook of Paper and Board**, (ed. H. Holik), Wiley-VCH Verlag, 2006.
156. E. Lehtinen. **Papermaking Science and Technology. Book 11. Pigment Coating and Surface Sizing of Paper**, Finnish Paper Association and TAPPI Press, Helsinki 1999.
157. W. Kogler, T. Gliese and W.J. Auhorn. Coating Pigments. In **Handbook of Paper and Board**, (ed. H. Holik), pp. 55–61, Wiley-VCH Verlag, 2006.
158. D.A. Hughes. Methods of Obtaining the Optical Properties of Papers Containing Titanium Dioxide and Mixtures of Titanium Dioxide and Other Fillers. *Tappi J.* 45(2):159A–163A, 1962.
159. G.A. Hemstock. The Effect of Clays Upon the Optical Properties of Paper. *Tappi J.* 45(2):158A–159A, 1962.
160. N.C. Debnath, and D.D. Kotkar. Theoretical Studies of Ligth Scattering Power. *Euro. Coat. J.* 4(1998):264–269, 1998.
161. W.D. Ross. Theoretical Light-Scattering Power of Tio2 Microvoids. *Ind. Eng. Chem. Prod. Res. Dev.* 13(1):45–49, 1974.
162. M. Kerker, D.D. Cooke and W.D. Ross. Pigmented Microvoid Coatings. Theoretical Study of Three Models. *J. Paint Technol.* 47(603):33–42, 1975.
163. W.D. Ross. Theoretical Computations of Light Scattering Power. Comparison between TiO2 and Air Bubbles. *J. Paint Technol.* 43(563):50–66, 1971.
164. S. Fitzwater and J.W. Hook III. Dependent Scattering Theory: A New Approach to Predicting Scattering in Paints. *J. Coatings Technol.* 57(721):39–47, 1985.
165. B.R. Palmer, P. Stamatakis, C.F. Bohren and G.C. Salzman. Multiple Scattering Model for Opacifying Particles in Polymer Films. *J. Coat. Technol.* 61(779):41–47, 1989.
166. B.J. Brinkworth. A Scattering Efficiency Factor for Radiative Transport. *J. Phys. D: Appl. Phys.* 5(3):476–480, 1972a.
167. J. Borch and P. Lepoutre. Light Reflectance of Spherical Pigments in Paper Coatings-a Comparison with Theory. *Tappi J.* 61(2):45–48, 1978.
168. E.S. Thiele and R.H. French. Light-Scatering Properties of Representative, Morphological Rutile Titania Particles Sutdied Using a Finite-Element Method. *J. Am. Ceram. Soc.* 81(3):469–479, 1998.
169. A. Penttilä, K. Lumme and L. Kuuti. Light-Scattering Efficiency of Starch

Acetate Pigments as a Function of Size and Packing Density. *Appl. Opt.* 45(15):3501–3509, 2006.
170. B.T. Draine and P.J. Flatau. Discrete-Dipole Approximation for Scattering Calculations. *J. Opt. Soc. Am. A* 11(4):1491–1499, 1994.
171. A. Penttilä. Private Communication. 2009.
172. S.-Y. Chang and W.E. Scott. An Investigation into the Mechanism of Titanium-Dioxide Extension by Calcium Carbonate. *Tappi J.* 71(10):128–131, 1988.
173. L. Abrams. Using Mercury Porosimetry to Characterize Coating Pore Structure and Its Relation to Coating Optical Performance. In *Tappi Coating Conference*, pp. 19–22, Nashville. TAPPI Press, Atlanta, 1996.
174. P.E. Pierce, S. Babil and J. Blasko. Hiding Power of Microvoids in Polymer Coatings. *Ind. Eng. Cem., Prod. Res. Develop.* 13(1):37–41, 1974.
175. J.T. Brown. The Relationship between Hollow Sphere Pigment Geometry and Optical Performance of Finished Paper Coatings. In *Tappi Coating Conference*, pp. 113–122, Montreal. TAPPI Press, Atlanta, 1991.
176. C.P. Hemenway, J.J. Latimer and J.E. Young. Hollow-Sphere Polymer Pigment in Paper Coating. *Tappi J.* 68(5):102–105, 1985.
177. T. Enomae and K. Tsujino. Application of Spherical Hollow Calcium Carbonate Particles as Filler and Coating Pigments. *Tappi J.* 3(6):31–49, 2004.

OPTICAL PROPERTIES OF PAPER: THEORY AND PRACTICE

Ramin Farnood

Department of Chemical Engineering and Applied Chemistry,
University of Toronto

Bob Pelton McMaster University

I do not have a question, I have a comment for the fraction of the paper physics community that does this kind of modelling. There is a real opportunity out there right now for doing modelling in this area, and it arises from a large number of biochemists who are doing biochemical tests on paper. In a typical biochemical test you generate a colour dye which you put in the spectrophotometer and use Beer's Law to get a concentration or you generate something that fluoresces and you measure fluorescent intensity and get a concentration. There are large numbers of people now trying to do this on paper surfaces. What is the role of paper roughness? What happens when these dyes diffuse down further into the paper structure? I think there is a real opportunity for modelling to quantify the coloured and fluorescent materials on paper surfaces. Just to finish this off and to give you an example, in the current issue of Analytical Chemistry there is an article where they talk about doing analysis on paper. They did their chemistry first, which generated a colour on paper, and then they saturated the paper with vegetable oil trying to contrast match the scattering of paper. Then they put it in a spectrophotometer. To me this is an act of desperation. What people really want to do is to be able to take a piece of paper with a colour generated by some biochemical test, point a cellphone camera at it, get a picture and send it off somewhere for external analysis. I think there is an opportunity here for modelling.

Ramin Farnood

Thank you for your comment, Bob, I agree with you. I think there is a lot that

we can do to improve the predictability of light–paper interaction specifically in the examples that you have just mentioned.

Jean-Francis Bloch University of Grenoble.

First of all, thank you very much for your very interesting presentation. I have to say I am a little bit confused when you say that the Kubelka-Munk model answers all technological problems. I have to say there are some limitations. At least the two coefficients you obtained (k and s) are only parameters from a given model. They are absolutely not physical parameters. Just to underline what Bob just said, if for example you increase dyes in a paper, you will of course modify the absorption coefficient (k), but you will also modify the scattering coefficient (s). People from time to time are surprised that the s coefficient only comes from the model that you have chosen and is not due to physical properties. So there are nowadays some alternatives to use, for example the radiative transfer equation with auxiliary functions – I will not go into the details. You also have new perspective to do this, such as to use diffusion models, for example. So I am a bit confused when you say, please just use Kubelka-Munk model, it works for everything. It has worked many times because you can use it for control, for example, and that is okay. You can use it as a first order to control the machine and it works quite well, but when you want to go further, it has a lot of limitations. Kubelka and Munk wrote be careful how you use the model and people just forget. It was only a comment, but I think that was important.

Ramin Farnood

Thank you for your comment, Jean-Francis. Actually I have read your paper with Jaques Silvey on this topic as well and I totally agree with you. I did not go through the details in my presentation. I have somewhere here made reference to the Foote effect which is what you pointed out, i.e. effect of dye on the scattering coefficient. Then as you have pointed out and I also presented here, scattering coefficient is not only a function of scattering cross-section but also absorption cross-section. So you are absolutely right. This is a deficiency of the Kubelka Munk model, but it is still widely used. The way I look at it, the value of a model is partly due to its simplicity and its ability to predict what we want to predict. As long as we are clear what the limitations are, as you pointed out, and we know how to interpret what we get out of the model, we are fine. The danger is when a model is used without an appreciation of the limitations of the model. I apologize if I perhaps made you believe that Kubelka Munk does everything. That is certainly not the case. I showed you

some example of Kubelka Munk applications, but we need to be aware of its limitations, and we need to be careful when we interpret the data.

Norayr Gurnagul FPInnovations (from the chair)

Perhaps I can just ask a simple question: can you make some comment about the use of CIE whiteness versus brightness, especially for paper makers out there?

Ramin Farnood

Okay, that is a controversial topic. I tried to make some comments in the manuscript and, if you like you can have a look at it in more detail, but what I understand is that brightness has been developed for a different purpose. It was developed originally to quantify the progress of a bleaching process and it does a fabulous job for that. But because it is simple and widely used for bleaching process, which by the way is focused very much on the blue region, it has also found application in paper. But, as you saw when I was talking about luminosity function, sensitivities are dependent on the wavelength of light and depending on the type of light source that was used, therefore, you may have a totally different perception, as published by Byron Jordan more than 10 years ago. Brightness is valuable but when we come to try to correlate it with human perception, the choice of illuminant, which in the brightness is limited to the blue region, would be very important as well.